

Summer 2018

## Impacts of Atmospheric Nitrogen Deposition and Coastal Nitrogen Fluxes on Chesapeake Bay Hypoxia

Fei Da

College of William and Mary - Virginia Institute of Marine Science, [fda@vims.edu](mailto:fda@vims.edu)

Follow this and additional works at: <https://scholarworks.wm.edu/etd>



Part of the [Marine Biology Commons](#), and the [Oceanography Commons](#)

---

### Recommended Citation

Da, Fei, "Impacts of Atmospheric Nitrogen Deposition and Coastal Nitrogen Fluxes on Chesapeake Bay Hypoxia" (2018). *Dissertations, Theses, and Masters Projects*. Paper 1530192498.

<http://dx.doi.org/10.25773/v5-y01d-4h22>

This Thesis is brought to you for free and open access by the Theses, Dissertations, & Master Projects at W&M ScholarWorks. It has been accepted for inclusion in Dissertations, Theses, and Masters Projects by an authorized administrator of W&M ScholarWorks. For more information, please contact [scholarworks@wm.edu](mailto:scholarworks@wm.edu).

Impacts of Atmospheric Nitrogen Deposition and Coastal Nitrogen Fluxes on  
Chesapeake Bay Hypoxia

---

A Thesis

Presented to

The Faculty of the School of Marine Science  
The College of William and Mary in Virginia

In Partial Fulfillment

of the Requirements for the Degree of  
Master of Science

---

by

Fei Da

May 2018

# APPROVAL PAGE

This thesis is submitted in partial fulfillment of  
the requirements for the degree of  
Master of Science

---

Fei Da

Approved by the Committee, February 2018

---

Marjorie A.M. Friedrichs, Ph.D.  
Committee Chair / Advisor

---

Courtney K. Harris, Ph.D.

---

Jian Shen, Ph.D.

---

Pierre St-Laurent, Ph.D.

---

Raleigh R. Hood, Ph.D.  
Horn Point Laboratory, University of Maryland Center for Environmental Science  
Cambridge, MD, USA

# TABLE OF CONTENTS

ACKNOWLEDGEMENTS.....	iv
ABSTRACT .....	v
1. INTRODUCTION .....	2
2. METHODS .....	4
2.1 CBP Available Data.....	4
2.2 <i>ChesROMS</i> -ECB Model Description.....	5
2.3 Nitrogen Inputs to <i>ChesROMS</i> -ECB.....	7
2.4 Model Experiments: Reference Run and Experimental Scenarios.....	10
3. RESULTS .....	12
3.1 Reference Run: Along-Bay Distributions and Skill Assessment .....	12
3.2 Sensitivity Experiments: Seasonal Results in the Mainstem Mesohaline Bay.....	14
3.3 Sensitivity Experiments: Along-Bay Results in Summer.....	14
3.4 Sensitivity Experiments: Dry vs. Wet Years .....	16
4. DISCUSSION .....	17
4.1 Overall Bottom Oxygen Response to Atmospheric and Coastal DIN Inputs .....	17
4.2 Seasonal Variability of Bottom Oxygen Response to Atmospheric and Coastal DIN Inputs.....	19
4.3 Interannual Variability of Bottom Oxygen Response to Atmospheric and Coastal DIN Inputs.....	20
4.4 Spatial Variability of Bottom Oxygen Response to Atmospheric and Coastal DIN Inputs.....	21
4.5 Future Work .....	22
5. SUMMARY AND CONCLUSIONS .....	23
Appendix A Modified <i>ChesROMS</i> -ECB Parameters.....	42
Appendix B <i>ChesROMS</i> -ECB Skill Assessment .....	42
REFERENCES .....	54

## ACKNOWLEDGEMENTS

There are many wonderful people who supported me during the completion of this thesis study. First of all, I'd like to express many thanks to my committee members for their helpful guidance and suggestions on my project and manuscript. In particular, my major advisor, Marjorie Friedrichs, is undoubtedly the most patient, knowledgeable and warm-hearted, unceasingly assisting me with writings, presentations and ways of thinking. Without her excellent mentoring and editing skills, I could not finish this thesis so smoothly. Pierre St-Laurent is like a co-advisor to me, extensively tutoring me in how to set up a numerical model, run jobs on high performance computer, and use MATLAB to analyze the model outputs. All the BioCOM members, including Julia Moriarty, Daniel Kaufman, Ike Irby, Jessie Turner, and Kyle Hinson have helped me with analytical and intellectual skills on my Masters research and coursework throughout the past two and half years. I would also like to thank the Chesapeake Bay Program Watershed Modeling group for providing the important riverine and atmospheric input files of our model experiments. Additionally, I'd like to thank the College of William and Mary high performance computer group for providing much technical support on computation resources. Financial support was from the Virginia Institute of Marine Science Office of Academic Studies, NASA Interdisciplinary Science Program (NNX14AF93G) and from the National Science Foundation (OCE-1259187). Furthermore, I want to thank the VIMS Chinese student community for offering help on apartment rental and vehicle purchase when I first arrived in the United States. Biggest thanks to my parents who always support my decisions and give endless love.

## ABSTRACT

Although rivers are the primary source of dissolved inorganic nitrogen (DIN) inputs to the Chesapeake Bay, direct atmospheric DIN deposition and DIN fluxes from the continental shelf can also significantly impact Chesapeake Bay hypoxia. The relative role of these additional sources of DIN has not previously been thoroughly quantified. In this study, the three-dimensional Estuarine-Carbon-Biogeochemistry model embedded in the Regional Ocean Modeling System (*ChesROMS-ECB*) is used to examine the relative impact of these three DIN sources. Model simulations highlight that DIN inputs from the atmosphere have roughly the same impact on hypoxia as the same gram for gram change in riverine DIN loading. DIN inputs from the shelf have a similar overall impact on hypoxia as those from the atmosphere ( $\sim 0.2 \text{ mg L}^{-1}$ ), however the mechanisms driving these impacts are different. While atmospheric DIN impacts dissolved oxygen (DO) primarily via the decomposition of autochthonous organic matter, coastal DIN also impacts DO via the decomposition of allochthonous organic matter entering the Bay from the continental shelf. The impacts of coastal and atmospheric DIN on estuarine hypoxia are greatest in the summer, and occur farther downstream (lower mesohaline) in wet years than in dry years (upper mesohaline). Integrated analyses of the relative contributions of all three DIN sources on summer bottom DO concentrations indicate that impacts of atmospheric deposition are largest in shallow near-shore regions, riverine DIN has dominant impacts in the largest tributaries and the oligohaline Bay, while coastal DIN fluxes are most influential in the polyhaline region. During the winter when estuarine circulation is strong and shelf DIN concentrations are relatively high, coastal DIN impacts bottom DO throughout the Bay.

Impacts of Atmospheric Nitrogen Deposition and Coastal Nitrogen Fluxes on  
Chesapeake Bay Hypoxia

# 1. Introduction

The Chesapeake Bay (Figure 1) is the largest and most productive estuary in the continental United States and plays a crucial role in watershed and coastal nitrogen transformations, transport and burial in the East Coast (Bronk et al., 1998; Kemp, 2005), but has been continually impacted by human activities ever since Europeans migrated to the region four centuries ago. Urbanization, industrial expansion and fertilizer usage are major factors contributing to the rapid increase of dissolved inorganic nitrogen (DIN) loads and concentrations in the Chesapeake Bay prior to the mid-1980s, which led to algal blooms and severe eutrophication (Nixon, 1995). One of the most serious issues caused by eutrophication and the resulting algal blooms is hypoxia, which is typically defined as dissolved oxygen concentration (DO) less than  $2 \text{ mg L}^{-1}$  (Seliger et al., 1985). In the Chesapeake Bay, hypoxia was first observed in the 1930s (Newcombe & Horne, 1938). Since the rapid increase of DIN loadings in the 1960s and 1970s, hypoxia has been observed every year in the Bay (Hagy et al., 2004; Bever et al. 2013). During the summer, the accelerating rate of microbial decomposition of organic matter increases oxygen consumption in both the water column and the sediments. Together with strengthened vertical stratification and reduced solubility, DO concentrations decrease, eventually resulting in hypoxia or even anoxia ( $\text{DO} < 0.2 \text{ mg L}^{-1}$ ) in deep bottom waters (Murphy et al., 2011). A study on Chesapeake Bay hypoxia using 3-D numerical models indicated that the volume of hypoxic water in the Bay ranged between 8-17  $\text{km}^3$  from 1985 to 2011 (Bever, et al., 2013). Within this large volume of low oxygen water, benthos struggle with hypoxic stress (Diaz and Rosenberg, 1995), and hypoxia-related diseases (Holland et al., 1987). For example, the abundance of benthos is typically low in hypoxic water, and sulfide accumulation in anoxic water is toxic to benthic invertebrates.

Over the past three decades, many management actions have been taken to try to reduce DIN inputs to the Bay from the watershed in order to reduce the harmful impacts of hypoxia. These have been met with mixed success. Due to the large land to water ratio (14:1), riverine DIN accounts for most of the DIN input to the Chesapeake Bay, and thus seasonal and long-term variability of water quality is highly sensitive to the amount of freshwater flow (Hagy et al., 2004; Kemp et al., 2005). Between World War II and the late 1980s, the nitrate ( $\text{NO}_3^-$ ) loading in the Susquehanna River increased by almost a



factor two (Harding et al., 2016). Because of the strenuous management efforts (e.g. the establishment of the Chesapeake Bay Total Maximum Daily Load), flow-adjusted  $\text{NO}_3^-$  loadings have been reduced by 5.4% since 1981 (Harding et al., 2016). However, projected climate change may be reducing the impact these riverine nutrient reductions are having on Chesapeake Bay hypoxia (Irby et al., 2017).

Atmospheric deposition is another important source of DIN for coastal waters of the US east coast (Paerl et al., 1999, 2002; St-Laurent et al., 2017). In the Chesapeake Bay, nearly half of the total atmospheric DIN deposition stemming from emission sources outside of the Bay watershed (USEPA, 2010a). Nitrate deposition is primarily from combustion of fossil fuels by industries and automobiles (Russell et al., 1998), while agricultural usage of fertilizers, farmed animal excreta, and biomass burning are primary contributors to anthropogenic ammonium ( $\text{NH}_4^+$ ) deposition (Prospero et al., 1996). Early studies indicated that total atmospheric nitrogen deposition, including both the “direct” component falling on Chesapeake Bay waters and the “indirect” component falling on land and being washed into the Bay, accounted for up to 40% of the total anthropogenic nitrogen loadings to the Chesapeake Bay during the mid-1980s (Fisher and Oppenheimer, 1991; Hinga et al., 1991). Encouragingly, the largest component of atmospheric DIN deposition, i.e.  $\text{NO}_3^-$ , has decreased up to 30% since 1985 due to the Clean Air Act, albeit with some interannual variability. In contrast, large increases in  $\text{NH}_4^+$  wet deposition (~40-50%) have been observed in Maryland and North Carolina since 1985 (Li et al., 2016). By the early 21<sup>st</sup> century, direct atmospheric deposition of DIN was reduced to roughly 10-15% of the total DIN inputs to the Chesapeake Bay (Linker et al., 2013).

Continental shelf waters with high DIN concentrations can be another potential source of nutrients to estuaries. In the Pacific Northwest, coastal upwelling provides a significant source of DIN to shallow shelf and estuarine waters (Hickey and Banas 2003; Brown and Ozretich, 2009; Davis et al., 2014). However, studies estimating DIN inputs from the continental shelf to the Chesapeake Bay are quite limited. Northeast winds during the summer could be upwelling favorable in the Middle Atlantic Bight (Blanton et al., 1985; Pietrafesa et al., 1994), bringing relatively high DIN concentration sub-surface shelf water to the adjacent region (Janowitz and Pietrafesa, 1982; Pietrafesa et al., 1994).

Cross-isobath fluxes of nutrient-rich waters (e.g. Labrador current) and winter mixing replenish the surface nutrient concentrations in Middle Atlantic Bight (Townsend et al., 2006). Williams et al. (2011) estimated that  $\text{NO}_3^-$  concentrations in the Middle Atlantic Bight were less than  $10.3 \text{ mmol-N m}^{-3}$  in depths  $<300 \text{ m}$ , and were greater than  $20.6 \text{ mmol-N m}^{-3}$  in denser waters at depths of  $300\text{-}500\text{m}$ , both of which are much higher than  $\text{NO}_3^-$  concentrations ( $<1 \text{ mmol-N m}^{-3}$ ) in surface waters near the mouth of the Chesapeake Bay. Although previous studies indicate that the Chesapeake Bay is likely a net source of DIN to the continental shelf (Kemp et al., 1997; Feng et al., 2015), DIN in continental shelf waters enters the Bay at depth via estuarine circulation, potentially impacting DO concentrations and primary production (PP) in the Bay.

In this study, a numerical model is used to better understand and quantify the relative magnitude of the impacts these three different sources of DIN have on primary production and hypoxia in Chesapeake Bay. By including all three sources of DIN (atmosphere, coastal ocean and rivers), a more realistic and reliable simulation of biogeochemical dynamics is conducted for the Chesapeake Bay. In Section 2 the data and models used in this study are described. Results of a four-year hindcast from 2002 to 2005 are presented in Section 3, along with the results of six sensitivity experiments in which each of the three different sources of DIN are increased/decreased independently in order to estimate their relative importance on primary production and DO. Seasonal, interannual and spatial differences in these impacts are discussed in Section 4, and the findings are summarized in Section 5.

## **2. Methods**

### **2.1 CBP Available Data**

A plethora of in situ data are available for model evaluation in the Chesapeake Bay. Most notably, the Chesapeake Bay Program (CBP) has been thoroughly monitoring Chesapeake Bay water quality since 1984. Available CBP biogeochemical data, generally measured once each month from October to March, and twice each month from April to September, include concentrations of DIN (here defined as the sum of  $\text{NO}_3^-$  and  $\text{NH}_4^+$ ), DO, dissolved organic nitrogen (DON), particulate organic nitrogen (PON), chlorophyll, total suspended solids (TSS) and surface diffuse attenuation ( $K_D$ ). Vertical profiles of DO

are measured at approximately 1m intervals throughout the water column; other variables are sampled at the surface and bottom, and at mid-level depths as well. In this study, model-data comparisons are focused on 18 main stem stations (Figure 1).

## 2.2 *ChesROMS-ECB* Model Description

A three-dimensional hydrodynamic-biogeochemistry model, *ChesROMS-ECB*, is used to address the above research questions pertaining to the impact of nitrogen inputs from the atmosphere and shelf. *ChesROMS-ECB* is an Estuarine-Carbon-Biogeochemistry (ECB) model embedded in the Regional Ocean Modeling System (ROMS) (Feng et al., 2015; Irby et al., 2016; Irby et al., 2017), and uses the *ChesROMS* grid of Xu et al. (2012).

Physical components of the model are from ROMS version 3.6 (Shchepetkin and McWilliams, 2005), which is a free-surface, terrain-following, primitive equation ocean model. Vertically, governing equations are discretized over a stretched terrain-following coordinates with 20 levels (Shchepetkin and McWilliams, 2005). The horizontal grid has orthogonal curvilinear coordinates with highest resolution (430m) in the northern Bay and lowest resolution (~10 km) at the open boundary in the southern end of Mid Atlantic Bight (Figure 1). Equations are discretized with a staggered Arakawa C-grid. The MPDATA (Multidimensional Positive Definite Advection Transport Algorithm) is applied to guarantee all variables at each time step are positive definite (Smolarkiewicz, 1983, 1984). The model was forced at the open boundary by tidal constituents from the Advanced Circulation (ADCIRC) model, and by observed non-tidal water levels from Duck, NC and Lewes, DE (Scully et al., 2016). Temperature, salinity and DO were nudged to the World Ocean Atlas monthly climatological data along the open boundary. Atmospheric forcing (e.g. 10m winds, short-wave radiation, rainfall, surface air humidity, air temperature and pressure) was derived from the North American Regional Reanalysis (NARR, Mesinger et al., 2006).

Although the ECB ecosystem module includes both nitrogen and carbon cycles, the work described here only involves the nitrogen component. This includes 11 state variables:  $\text{NO}_3^-$ ,  $\text{NH}_4^+$ , phytoplankton, zooplankton, small and large detritus, semilabile and refractory dissolved organic nitrogen, inorganic suspended solids (ISS), DO and chlorophyll (Feng et al., 2015). The original *ChesROMS-ECB* model has been shown to

simulate Chesapeake Bay hydrodynamics and biogeochemical processes quite well (Feng et al., 2015); however, a number of modifications have been subsequently made to the original equations and parameter choices in order to improve model-data agreement. These are described in detail below.

To improve model-data comparisons for oxygen concentrations and primary production in the lower Chesapeake Bay, the light attenuation formulation in *ChesROMS-ECB* was reassessed. Specifically, an underestimation of light attenuation in the lower Bay was causing an overestimation of primary production and oxygen. Historical CBP observations suggested that this was at least partially because the model was underestimating observed ISS. As a result, a 4 mg L<sup>-1</sup> ISS washload was added throughout the Bay. In addition, the factor converting organic suspended solids from g-C m<sup>-3</sup> to g m<sup>-3</sup> was changed to 2.9 (Cercio et al., 2017). Because the historical CBP observations indicated that the lowest 25<sup>th</sup> percentile of K<sub>D</sub> in the lower Chesapeake Bay ranges from 0.55 - 0.75 m<sup>-1</sup>, the minimum allowed value for K<sub>D</sub> was set to 0.6 m<sup>-1</sup>, as in Irby et al. (2017). Finally, the Jerlov water type (Paulson and Simpson, 1977; Jerlov, 1976) was increased to coastal waters (type 3).

To replicate the seasonal cycles of biogeochemical variables in *ChesROMS-ECB* more realistically, temperature dependence was added to multiple biogeochemical processes, such as phytoplankton growth rate, zooplankton grazing rate, and the decomposition rate of organic matter (Table A1). Lomas et al. (2002) studied phytoplankton growth rates in the Chesapeake Bay, and demonstrated that phytoplankton at low temperatures (T<20°C) tend to maintain a constant growth rate, whereas the phytoplankton community tends to follow an exponential growth rate with a natural log Q<sub>10</sub> of 1.62 at warmer temperatures (Q<sub>10</sub> is a measure of the temperature sensitivity of a biological/chemical reaction rate due to an increase in temperature by 10 °C.). Zooplankton grazing is another highly temperature dependent estuarine process. A function based on a natural log Q<sub>10</sub> of 2.1 was chosen, which is derived from the community respiration study in Lomas et al. (2002). In addition, remineralization and solubilization are important microbial activities that account for the decomposition of detrital nitrogen and carbon in *ChesROMS-ECB*. Like metabolic activities of most organisms, bacterial productivity undergoes an exponential relationship with

environmental temperature, due to enzyme activity in the Chesapeake Bay (Shiah and Ducklow, 1994). The detrital nitrogen and carbon remineralization and solubilization rates were thus modified from constant values to rates with temperature coefficients (Q10) equal to 2.1 (Lomas et al., 2002). All parameterization changes were tested independently at first, and then were integrated together for evaluations with in situ CBP data (Section 2.1).

### **2.3 Nitrogen Inputs to *ChesROMS-ECB***

In an attempt to generate more realistic simulations of nitrogen cycling within the Chesapeake Bay, nitrogen inputs to the Bay were re-examined. Primary modifications from Feng et al. (2015) include: (i) using watershed nitrogen inputs from the CBP Watershed Model, (ii) nudging to oceanic  $\text{NH}_4^+$  and  $\text{NO}_3^-$  data along the coastal open boundary, and (iii) including atmospheric nitrogen deposition. These three inputs are described in detail below.

#### **2.3.1 Terrestrial Inputs**

As in Irby et al. (2017) watershed inputs of freshwater, nitrogen and inorganic sediment (including both point source and non-point source inputs) are derived from the Phase 5.3.2 CBP Watershed Model (CBWM; Shenk and Linker, 2013). The CBPWM includes about one thousand model segments with an average size of  $170 \text{ m}^2$ , 237 hydrology calibration stations, and 13 types of land use that change hourly with time (USEPA, 2010b). Simulated hydrology and water quality variables are calibrated using station measurements (USEPA, 2010c).

In this study, daily estimates of CBPWM freshwater flow,  $\text{NH}_4^+$ ,  $\text{NO}_3^-$ , DON and sediments were used as terrestrial inputs to *ChesROMS-ECB*. Median values of CBPWM DIN ( $\text{NH}_4^+ + \text{NO}_3^-$ ) inputs to the Bay range from  $\sim 400 \times 10^6 \text{ g-N d}^{-1}$  during the spring freshet, to  $\sim 100 \times 10^6 \text{ g-N d}^{-1}$  in the summer (Figure 2a), with large interannual variability for the four study years (2002-2005, Table 1). Semi-labile DON inputs were computed as the total biological oxygen demand plus 80% of the phytoplankton nitrogen. The refractory DON input was set to be 40% of the total refractory organic nitrogen from the CBPWM. The rest of the refractory organic nitrogen (60%) and phytoplankton nitrogen (20%) was assumed to enter the Bay as particulate organic nitrogen. Although

carbon cycling was not the focus of this study, carbon inputs (dissolved and particulate organic carbon, dissolved inorganic carbon) were obtained from Tian et al. (2015).

### **2.3.2 Atmospheric Inputs**

Because direct atmospheric deposition of DIN accounts for a significant fraction of the total DIN inputs to the Chesapeake Bay (Linker et al., 2013), an important model improvement was to include this as a source of DIN to the estuary. As is the case for the CBP's Water Quality Sediment Transport Model (Cerco, 2017), estimates of atmospheric DIN deposition were obtained from a combination of two different models: a regression model for wet deposition (Grimm and Lynch, 2005; Grimm, 2017) and a continental-scale Community Multiscale Air Quality model (CMAQ version 5.0.2, Appel et al., 2013; Gantt et al., 2015; St-Laurent et al., 2017) for dry deposition. Because the concentration of DON in wet deposition ( $50 \text{ mg m}^{-3}$ , Keene et al. 2002) over the Bay is much smaller than that of DIN ( $400\text{-}500 \text{ mg m}^{-3}$ , USEPA 2010a), DON deposition is assumed to be negligible as in Grimm (2017).

Wet atmospheric deposition estimates used in this study were provided by the CBP. Specifically, their Phase 6 regression model for wet nitrogen deposition (Grimm 2017) was refined from previous versions developed for the Chesapeake Bay watershed (Grimm and Lynch, 2005) by taking local emissions (i.e. local livestock production and fertilizer application to cropland) into consideration. Overall, the model development focused primarily on using long-term and seasonal trends in precipitation chemistry (i.e.  $\text{NH}_4^+$  and  $\text{NO}_3^-$  concentrations, precipitation volume), land use, and local emission data as predictors selected for a stepwise linear least squares regression model (Grimm 2017). Daily precipitation records over 1984-2014 were collected from 85 of the National Atmospheric Deposition Program, the National Trends Network, and the Pennsylvania Atmospheric Deposition Monitoring Network stations. In addition, Grimm (2017) used local land usage information from National Land Cover Data, local ammonia ( $\text{NH}_3$ ) and nitrous oxide ( $\text{NO}_x$ ) emissions from the National Emission Inventory database to improve the accuracy of daily  $\text{NH}_4^+$  and  $\text{NO}_3^-$  wet deposition estimates. The daily wet DIN deposition rates were first calculated within the cells of a uniform 5km grid overlaying the Chesapeake Bay Watershed Model region, and then area-weighted to each land modeling segment or water quality management unit polygon employed by the

Phase 6 Watershed Modeling Program. As part of this study, the segments positioned over the Chesapeake Bay surface water were used to provide estimates of wet deposition for each *ChesROMS*-ECB grid cell using the nearest-neighbor method.

Monthly averaged dry DIN deposition estimates were obtained from CMAQ, an open-source numerical air quality model that simulates the atmospheric transport, chemical reactions and emissions of various airborne gases, particles and pollutants. The meteorological information derived from the Weather Research and Forecasting model (WRF 3.4. Skamarock et al., 2008) and CB05TU chemistry mechanisms (Sarwar et al., 2013) are required inputs for CMAQ. The horizontal resolution of the  $\text{NH}_4^+$  and  $\text{NO}_3^-$  deposition fields is 12 km. The CMAQ grid points positioned over the Chesapeake Bay surface water were used for providing estimates of dry deposition for each *ChesROMS*-ECB grid using the nearest-neighbor method. This monthly dry atmospheric deposition of DIN was then downscaled to daily inputs through linear interpolation. On average, dry plus wet atmospheric deposition of DIN accounts for ~10% of the riverine DIN inputs to the Chesapeake Bay, with this percentage being highest during dry years (e.g. 2002; Table 1) and in dry times of year (i.e. summer; Figures 2a and 2b).

### **2.3.3 Coastal Inputs**

In this study, a passive-active open boundary condition (RadNud, Marchesiello et al., 2001) is used for temperature, salinity,  $\text{NH}_4^+$ ,  $\text{NO}_3^-$ , oxygen and dissolved organic nitrogen (DON). When fluxes are directed outward across the boundary, the model employs a radiation condition (passive), which is derived from a two-dimensional wave equation. As a result, the radiation boundary condition is calculated from the interior solution, propagating through the boundary as a wave. However, when fluxes are directed into the model domain from outside the boundary, the model employs a nudging condition (active). In this case the model results within the nudging region are nudged towards externally specified tracer concentrations with a nudging time scale of 15 hours. This combined radiation-nudging boundary condition is sufficient for maintaining stability (Marchesiello et al., 2001).

To improve the realism of simulated inorganic nitrogen exchange with the continental shelf, *ChesROMS*-ECB was nudged to oceanic  $\text{NH}_4^+$  and  $\text{NO}_3^-$  data along the outer boundary of the model domain (Figure 1), in the Mid Atlantic Bight. In situ  $\text{NH}_4^+$

and  $\text{NO}_3^-$  data were obtained from the Ocean Acidification Data Stewardship Project (OADS) datasets (<https://www.nodc.noaa.gov/oceanacidification/data/>; 22 cruises from 2009 - 2016) and cruise data (Filippino et al., 2009; five cruises from 2005 - 2006) within the domain  $35.8^\circ\text{-}38.5^\circ\text{N}$ ,  $74.1^\circ\text{-}76.0^\circ\text{W}$ . Because the in situ data were sparsely distributed in time over the past decade, they were averaged to obtain monthly  $\text{NH}_4^+$  and  $\text{NO}_3^-$  climatologies for the months when the most data were available: February, May, June, August and November. Since the distribution of measurements was also spatially sparse,  $\text{NH}_4^+$  and  $\text{NO}_3^-$  data were horizontally averaged over the model open boundary, but vertical variations were retained. The  $\text{NH}_4^+$  and  $\text{NO}_3^-$  data in each of the five months were gridded onto standard 5-10m depth intervals to obtain vertical  $\text{NH}_4^+$  and  $\text{NO}_3^-$  profiles. These vertical profiles were then linearly interpolated to the bottom of the model grid. Only data from the upper 40m of the water column was used for nudging, to assure consistency with the bathymetry along the model open boundary. Finally, to obtain a complete seasonal cycle of DIN along the open boundary (Figure 2c), the existing five months of data were interpolated to cover the full year.

In addition to nudging modeled DIN concentrations to observations at the open boundary, model estimates of dissolved organic matter were also nudged to observed estimates. Refractory DON concentrations along the open boundary were nudged to a value of  $3.3 \text{ mmol-N m}^{-3}$ , assuming refractory dissolved organic carbon (DOC) concentrations of  $50 \text{ mmol-N m}^{-3}$  and a C:N ratio of 15:1 (Fisher et al., 1998). Semilabile DOC concentrations were estimated by subtracting the constant refractory DOC ( $50 \text{ mmol-N m}^{-3}$ ) from estimates of total DOC derived from a satellite DOC algorithm developed for the Middle Atlantic Bight (Mannino et al., 2016). Finally, a C:N ratio of 12:1 was used to estimate semilabile DON concentrations along the open boundary (Feng et al., 2015).

#### **2.4 Model Experiments: Reference Run and Experimental Scenarios**

A reference simulation was conducted to represent January 2001 to December 2005, incorporating nitrogen inputs from all three sources (watershed, atmosphere and coastal ocean). The first year was considered to be a spin up year, and only 2002-2004 results were analyzed. These specific four years were chosen, as they represent a



combination of dry (2002), wet (2003-2004) and normal (2005) years, and because CMAQ results (St-Laurent et al., 2017) are not available prior to 2002.

This reference simulation was compared to the results of three sensitivity experiments (AtmN, CoastalN,  $\Delta$ RiverN; Table 2) in order to assess the relative impact of nitrogen from all three sources on primary production and oxygen concentrations in Chesapeake Bay (Table 2). Specifically, the sensitivity experiments included turning off and doubling atmospheric nitrogen deposition (AtmN) and setting the DIN concentrations along the open boundary to zero and 200% of the baseline concentrations used in the reference run (CoastalN). To quantify the relative impacts of DIN from the atmosphere and continental shelf to those from the rivers, a set of riverine DIN experiments was also conducted ( $\Delta$ RiverN). These included reducing and increasing the riverine DIN loadings by the same amounts as was done in the atmospheric deposition experiments via modifying the daily riverine DIN concentrations, but keeping the freshwater discharge the same. Thus in 2002, riverine DIN was reduced by  $\Delta = \text{atmospheric inputs/riverine inputs} = 10.5\%$  (Table 2), whereas in 2003 riverine DIN was reduced by  $\Delta = 7.7\%$  (Table 2). All experiments were run from 1 January 2001 to 31 December 2005, as in the reference simulation.

A RGB (Red, Green Blue) primary color diagram was used to assist with visualization of the impacts of all three sensitivity experiments simultaneously. In each model grid cell (i,j), the changes in bottom DO resulting from the AtmN experiments are averaged and assigned to variable “R”. Similarly, the averaged impact due to the  $\Delta$ RiverN experiments is set to “G”, and the differences caused by the CoastalN experiments is set to “B”. Then R, G or B is each normalized to the maximum value among them (e.g.  $R' = R/\max(R, G, B)$ ). The color of the grid cell (i,j) was then represented by the combination of these three numbers R', G' and B' (Figure 3). In this way, the RGB color of each grid cell within the model domain is calculated to illustrate the relative impacts of all three sensitivity experiments over the entire Chesapeake Bay. As the triangle color bar indicates (Figure 3), red represents a 100% impact from atmospheric DIN deposition, while white means all three experiments are equally important in explaining the estimated changes in bottom DO.

### 3. Results

#### 3.1 Reference Run: Along-Bay Distributions and Skill Assessment

To evaluate model skill, results from the reference run were extensively compared, both qualitatively and quantitatively, to CBP observations along a transect down the main channel of the Chesapeake Bay (Figure 1). Quantitative skill metrics (Hofmann et al., 2008; Jolliff et al., 2009) were applied to evaluate how well the reference run reproduced the available data and were described in Section 2.1 (Appendix A). Model simulations and observations at the same temporal and spatial locations were compared to achieve point-to-point comparisons. Qualitatively, the salinity field is well captured by the model in both summer and winter (Figure 4a and 4b) along the entire mainstem transect, i.e. throughout the oligohaline (defined as region with average surface salinity < 5psu), mesohaline (5 psu < surface salinity < 15 psu), and polyhaline (surface salinity > 15 psu).

The along-Bay DIN pattern is reproduced well throughout the Bay, though minor discrepancies exist (Figures 4c and 4d). DIN concentrations peak at the head of the Bay ( $\sim 80\text{-}100 \text{ mmol-N m}^{-3}$ ) and decrease downstream, reaching concentrations less than  $10 \text{ mmol-N m}^{-3}$  at the Bay mouth. Overall, summer DIN is  $\sim 20 \text{ mmol-N m}^{-3}$  lower than that in the winter. In both seasons, the model successfully reproduces the observed well-mixed conditions in the oligohaline Bay, with only minor overestimates of summer DIN (by  $\sim 10 \text{ mmol-N m}^{-3}$ ). In the upper mesohaline Bay, modeled DIN concentrations agree with observations well in the upper water column, but slightly underestimate the vertical gradients of DIN in the winter (Figure 4d). Throughout the lower mesohaline and polyhaline Bay, the model simulates the spatial structure of DIN very well in both the summer and winter.

Model estimates of DON and PON reproduce the mainstem CBP observations relatively well, though concentrations are slightly too high in the summer and too low in winter (Figures 4e-4f). Observed concentrations of DON are highest in the mesohaline Bay in both seasons with relatively small vertical gradients. Modeled DON agrees with DON concentrations and the vertical structures in the polyhaline Bay relatively well in both seasons (Figures 4e and 4f). However, the model underestimates the maximum DON concentrations in the mesohaline Bay at some stations by up to  $5 \text{ mmol-N m}^{-3}$ , and

overestimates DON in the upper Bay by  $\sim 3 \text{ mmol-N m}^{-3}$  in the summer, and the bias goes up to  $10 \text{ mmol-N m}^{-3}$  in the winter. PON, defined in the model as phytoplankton + zooplankton + detritus, is generally higher at the surface (Figures 4g and 4h) where light stimulates phytoplankton growth, except in the upper Bay where high inorganic sediment concentrations reduce light availability and thus DIN remains high (Figures 4c and 4d). Model reproduces summer PON very well throughout the Bay, with only a  $\sim 5 \text{ mmol-N m}^{-3}$  bias in the surface mesohaline waters. In the middle Bay, summer PON has a sharp vertical gradient, which is also well captured by the model. During the winter, the model underestimates PON throughout most of the Bay, however the evenly distributed horizontal and vertical structure of PON is reproduced successfully.

The model simulates the distribution of observed oxygen well throughout the water column (Figures 4i and 4j). The four-year average of modeled oxygen concentrations range between  $1\text{-}9 \text{ mg L}^{-1}$  and  $8\text{-}13 \text{ mg L}^{-1}$  in the summer and winter, respectively. In both the model results and the observations, the vertical gradient during the summer is much larger than that in the winter, and is larger in the mid-Bay than the upper or lower Bay, agreeing well with temporally averaged measurements in both seasons. Although there is a minor bias ( $1\text{-}2 \text{ mg L}^{-1}$ ) between the model and observation in the surface water of the mesohaline Bay in the summer, the subsurface oxygen concentrations and sharp vertical gradients are both simulated well. During the winter, DO concentrations and vertical gradients are captured well by the model in most of the Bay, although modeled bottom DO concentrations are biased high ( $\sim 1 \text{ mg L}^{-1}$ ) in the deepest portions of the mainstem. Most notably, the model successfully captures the large volume of hypoxic water in the deep trench during the summer.

Modeled primary production is highest at the surface (up to  $2000$  and  $300 \text{ mg-C m}^{-3} \text{ d}^{-1}$  in the summer and winter, respectively) and decreases exponentially to zero within the first  $3\text{-}10$  meters of the water column in both seasons (Figures 4k and 4l). In the lower Bay, primary production penetrates deeper in to the water column than the upper and middle Bay throughout the year. Summer primary production peaks in the mesohaline Bay where nutrients and light are both sufficient for growth (Harding et al., 2002), while surface production in the winter is the greatest in the lower Bay. Although primary production data are not available in the CBP Water Quality Monitoring database,

the modeled estimates are qualitatively consistent with other in situ data (Harding et al., 2002) and satellite estimates (Son et al., 2014).

### **3.2 Sensitivity Experiments: Seasonal Results in the Mainstem Mesohaline Bay**

Each of the three DIN sources to the Chesapeake Bay, i.e. atmospheric deposition, coastal inputs and riverine loading, causes varying impacts on depth-averaged DIN concentrations, depth-integrated primary production and bottom DO within the mainstem mesohaline region of the Bay where hypoxia is of greatest concern. In this region, the  $\Delta$ RiverN experiment results in the largest influence on four-year averaged DIN concentrations of all three sensitivity experiments (Table 3). In terms of annual average primary production, the AtmN and  $\Delta$ RiverN experiments have greater impacts than the experiment with modified coastal DIN inputs, for both absolute and percent difference (Table 4). In contrast, the CoastalN experiment results in slightly greater changes in annual average bottom DO concentrations than either of the other two experiments (Table 5).

Overall, the three sensitivity experiments cause differences in production and bottom DO that are largest in the summer (Tables 4 and 5), while the impact on depth-averaged DIN concentrations are greatest in the spring and/or winter (Table 3). The summertime changes in depth-integrated primary production in this mainstem mesohaline region are relatively low: 2.6%, 3.3% and 1.1%, resulting from the AtmN,  $\Delta$ RiverN and CoastalN experiments respectively (Table 4), while changes in depth-averaged spring DIN concentrations are somewhat higher: 4.8%, 8.4% and 3.7% for the AtmN,  $\Delta$ RiverN and CoastalN experiments respectively (Table 3). During other seasons of the year, the percent change in bottom DO resulting from these sensitivity experiments is much lower (< 2%) than those in the summer (~9% for all three experiments, Table 5). For this reason, the following sections focus on providing a more detailed examination of the sensitivity experiment results occurring in summer.

### **3.3 Sensitivity Experiments: Along-Bay Results in Summer**

In general, the AtmN, CoastalN and  $\Delta$ RiverN experiments cause qualitatively similar impacts on water column DIN concentrations in the summer, though the spatial structures of these responses differ slightly (Figure 5). The AtmN experiment causes quite uniform changes in water column DIN concentrations horizontally and vertically

(2-4 mmol-N m<sup>-3</sup>), except in the polyhaline region where little change occurs (Figures 5a and 5b). The  $\Delta$ RiverN experiment results in relatively large differences in mainstem DIN (up to 6-8 mmol-N m<sup>-3</sup>) in the uppermost 50 km of the Bay, but these changes decrease downstream, reaching 2-4 mmol-N m<sup>-3</sup> throughout the mesohaline Bay and nearly zero in the polyhaline regions (Figures 5c and 5d). The CoastalN experiment causes a larger impact on DIN in deeper waters (2-3 mmol-N m<sup>-3</sup>), and a smaller impact in shallow waters above the pycnocline. In addition, it has almost no influence in the upper oligohaline Bay (Figures 5e and 5f).

The impacts of the sensitivity experiments on primary production are concentrated in the uppermost five-meters of the water column, and are of the same order of magnitude for all three experiments. As expected, increases and decreases in DIN inputs result in increases and decreases in primary production, respectively (Figure 6). In the turbidity maximum zone, primary production barely changes regardless of which DIN input is modified. Both the AtmN and  $\Delta$ RiverN experiments cause 60-80 mg-C m<sup>-3</sup> d<sup>-1</sup> differences in primary production throughout the middle Bay, and result in 20-40 mg-C m<sup>-3</sup> d<sup>-1</sup> changes in the lower Bay. However, the  $\Delta$ RiverN experiment has a slightly greater impact in the middle Bay and the AtmN experiment results in a little more primary production in the lower Bay. Although the CoastalN impacts production less than either of the other two experiments in the upper mesohaline Bay, it causes larger and deeper changes in primary production throughout the lower Bay (~50 mg-C m<sup>-3</sup> d<sup>-1</sup> and ~10m, respectively).

Dissolved oxygen is changed by up to 0.3 mg L<sup>-1</sup> in the summer for all three sensitivity experiments (Figure 7). Generally if DIN inputs are reduced, DO decreases at the surface and increases below the pycnocline, and vice versa. Both the AtmN and  $\Delta$ RiverN experiments cause a ~0.1 mg L<sup>-1</sup> change in surface DO in the lower mesohaline and polyhaline Bay, while a smaller increase is observed in the CoastalN experiments. Below the pycnocline, DO concentrations barely change in the oligohaline Bay regardless of which DIN input is modified, however in the mesohaline Bay changes of 0.1-0.3 mg L<sup>-1</sup> result from each experiment. Specifically, the impacts on DO are greatest in the deep trench (up to 0.3 mg L<sup>-1</sup>). Most notably, the CoastalN experiment impacts DO ~0.1 mg L<sup>-1</sup>.

<sup>1</sup> less in the upper mesohaline Bay and  $\sim 0.1 \text{ mg L}^{-1}$  more in the polyhaline region than either of the other two experiments.

Overall, the three sensitivity experiments have an equally important influence on the cumulative hypoxic volume (CHV) of the Chesapeake Bay (Table 6). (CHV is calculated by integrating the volume of all grid cells with DO less than a certain threshold concentration, e.g.  $5 \text{ mg L}^{-1}$ , as described in Bever et al. (2013)). In general, the impact on CHV resulting from the AtmN and  $\Delta$ RiverN experiments becomes larger than that from the CoastalN experiment as the DO threshold defining "hypoxia" is decreased. For example, at  $\text{DO} < 5 \text{ mg L}^{-1}$ , modifying either atmospheric or riverine DIN inputs impacts CHV less than altering the coastal DIN inputs (by  $1\text{-}2 \text{ km}^3 \text{ d}$ ); this has a larger impact in the polyhaline Bay where DO concentrations are relatively high (Figure 4i). However, at  $\text{DO} < 0.2 \text{ mg L}^{-1}$ , the AtmN and  $\Delta$ RiverN experiments have 4% and 7% greater impacts on CHV than does the CoastalN experiment, respectively, since these lowest DO concentrations occur in the mesohaline Bay far from the coastal boundary (Figure 4i).

### **3.4 Sensitivity Experiments: Dry vs. Wet Years**

The impact of changes in nitrogen inputs on mainstem DIN concentrations can depend on whether a year is particularly dry (e.g. 2002) or wet (e.g. 2003). Depth-averaged DIN concentrations are examined here since the impacts of both surface (AtmN and  $\Delta$ RiverN) and bottom DIN (CoastalN) sources are studied. In the AtmN and CoastalN experiments, differences in depth-averaged DIN concentrations along the mainstem are relatively evenly distributed throughout the Bay ( $0\text{-}1.5 \text{ mmol-N m}^{-3}$ ), and are similar for both dry and wet years (Figures 8a and 8c). The impact on DIN along the mainstem resulting from the  $\Delta$ RiverN experiment peaks in the upper Bay ( $\sim 300 \text{ km}$  away from the Bay mouth) and generally decreases to nearly zero in the lower Bay in both dry and wet years (Figure 8b). In contrast to the other two sensitivity experiments, in the upper Bay, the  $\Delta$ RiverN experiment results in a  $\sim 4 \text{ mmol-N m}^{-3}$  greater difference in the dry year compared to the wet year (Figure 8b).

In the wet year, the largest changes in depth-integrated primary production resulting from the AtmN and  $\Delta$ RiverN experiments are farther downstream than those in the dry year (Figures 8d and 8e). The CoastalN experiment, however, demonstrates smaller differences in impacts in dry vs. wet years (Figure 8f; Table 7). Depth-integrated

primary production increases up to 150 and 180 mg-C m<sup>-2</sup> d<sup>-1</sup> in the mesohaline Bay during a dry year for the AtmN and ΔRiverN experiments, respectively, both decreasing upstream to zero in the turbidity maximum zone. On the contrary, these maximum changes in primary production resulting from atmospheric and riverine inputs are located in the polyhaline Bay in the wet year (~100 mg-C m<sup>-2</sup> d<sup>-1</sup>). Regardless of dry or wet conditions, the CoastalN experiment has almost no impact on depth-integrated production in the upper mesohaline and oligohaline Bay (Figures 8f and 8e). However, its impacts increase gradually along the mainstem to ~200 mg-C m<sup>-2</sup> d<sup>-1</sup> in the polyhaline Bay, with slightly greater changes in the dry year (Figure 8f).

The maximum impact on summer bottom DO from all three sensitivity experiments occurs in the middle Bay during the dry year, whereas it is located farther downstream in the lower Bay in the wet year (Figures 8g-8i). Specifically, for both the AtmN and ΔRiverN experiments, bottom DO is impacted by up to 0.3 mg L<sup>-1</sup> in the middle Bay in the dry year, but the impacts are smaller (~0.15 mg L<sup>-1</sup>) and farther south in the wet year. The CoastalN experiment results in slightly smaller changes in bottom DO (up to 0.2 mg L<sup>-1</sup>) in the dry year; however, in the wetter year, the differences in bottom DO due to coastal DIN inputs reach up to 0.3 mg L<sup>-1</sup> at the mouth of the Bay. Overall, regardless of whether a year is particularly dry or wet, the results from the AtmN and ΔRiverN sensitivity experiments are very similar throughout the Bay, whereas the CoastalN experiment results in a greater impact in bottom DO in the polyhaline Bay (0.1-0.2 mg L<sup>-1</sup>), and a smaller impact in the middle Bay (~0.1 mg L<sup>-1</sup>) compared to the other two scenarios.

## **4. Discussion**

### **4.1 Overall Bottom Oxygen Response to Atmospheric and Coastal DIN Inputs**

Atmospheric DIN deposition is a crucial source of nutrients entering the Chesapeake Bay, and causes nearly the same impact on hypoxia as the same amount of riverine DIN loading. Direct atmospheric DIN deposition fuels an additional ~100 mg-C m<sup>-2</sup> d<sup>-1</sup> of primary production during the summer in the nutrient-limited mesohaline Bay (Figure 6b and 8d), providing more organic material as substrate for microbial decomposition and decreasing DO concentrations by up to 0.3 mg L<sup>-1</sup> (Figure 7b and 8g).

Similarly, decreasing riverine DIN loading by ~10% has roughly the same impact as eliminating atmospheric DIN deposition, on reducing bottom oxygen concentrations (Table 5) and cumulative hypoxic volume (Table 6) in the hypoxia-prone mainstem. In particular, because the average of atmospheric DIN deposition is roughly equal to ~10% of riverine DIN inputs (Figure 2), direct atmospheric DIN deposition causes nearly the same impact on hypoxia as the same gram for gram change in riverine DIN loading. Since DIN inputs represent ~60% of the total nitrogen (TN) entering from the watershed, a 1.0 GgN reduction in atmospheric DIN deposition has essentially the same impact on hypoxia as reducing 1.6 GgN of TN inputs from the watershed. This is critical information for coastal resource managers who must assess impacts of changes in atmospheric and riverine nitrogen loading to the Bay.

Coastal DIN inputs are also critical for understanding trends in Chesapeake Bay hypoxia, and generally cause a similar impact on oxygen concentrations as direct atmospheric DIN deposition, even though the net flux from of DIN through the Chesapeake Bay mouth is directed from the Bay to the shelf (Table 7). DIN from the coastal ocean has a smaller impact than atmospheric DIN on summer primary production in the mesohaline Bay ( $\sim 50 \text{ mg-C m}^{-2} \text{ d}^{-1}$ ; Figures 6f and 8f), since coastal DIN enters the Bay at the bottom of the water column via estuarine circulation whereas DIN from the atmosphere enters at the nutrient-limited surface. However, higher coastal DIN concentrations on the shelf result in greater coastal phytoplankton growth, and ultimately more allochthonous organic matter input entering through the Bay mouth. As a result, more oxygen is consumed when this additional organic matter is remineralized in the Bay at depth. Thus, although the in situ mesohaline primary production is greater when additional DIN enters from the atmosphere rather than from the coast (Table 4), the additional organic matter provided by allochthonous inputs from the coast causes the impact on bottom DO to be comparable in both cases (Table 5), regardless of whether the source of extra nitrogen is from the atmosphere or the shelf. Therefore, atmospheric and coastal DIN inputs are both crucial sources of nutrients that impact Chesapeake Bay oxygen dynamics.



## **4.2 Seasonal Variability of Bottom Oxygen Response to Atmospheric and Coastal DIN Inputs**

The impacts of changing atmospheric and coastal DIN inputs on primary production are modulated seasonally by both physical and biogeochemical processes. In summer, a combination of high temperatures and abundant solar radiation promotes the growth of phytoplankton (Kremer and Nixon, 1978), resulting in high rates of primary production (Figure 4). Furthermore, strong spring river discharge results in strengthened stratification in the summer (Scully, 2013), which helps to keep highly productive surface layers from being mixed with more light limited sub-pycnocline water, maintaining the high surface production. As a result, the surface waters of the mesohaline Bay are depleted of nitrogen (Kemp et al., 2005), and thus primary production is very sensitive to changes in DIN inputs from the atmosphere and shelf during the summer (Table 4, Figure 6). The considerable increase in production during the summer caused by the added DIN also results in more organic material being available for microbial decomposition and ultimately enhanced oxygen consumption (thereby reducing oxygen concentrations) throughout the summer (Table 5, Figure 7). Because DIN inputs are immediately taken up by the resident nutrient-limited phytoplankton community at this time of year, DIN concentrations, in contrast, are not as strongly impacted by these summer inputs in the mesohaline Bay (Figure 5), but are more strongly impacted by additional inputs in spring when nitrogen is not as limiting (Table 3).

In the winter, low temperatures and light are the primary reason for the small change in primary production resulting from changes in DIN inputs. Phytoplankton growth rate in the winter is much lower than that in the summer (Eppley, 1972), and light limitation is stronger in the winter due to deeper vertical mixing (Fisher et al., 1999). As a result, the impacts of new sources of DIN on primary production are smallest in winter (Table 4), whereas the impact on depth averaged DIN concentration is relatively high (Table 3) since very little of these additional DIN inputs is assimilated into organic matter at this time of year. This is true despite the fact that shelf DIN concentrations are highest in the winter (Figure 2c). These limited changes in primary production coupled with the low microbial degradation rates due to the cold temperatures cause minimal changes in bottom DO resulting from DIN inputs in winter throughout the mainstem Bay.

### **4.3 Interannual Variability of Bottom Oxygen Response to Atmospheric and Coastal DIN Inputs**

Although the impact of atmospheric DIN deposition on DIN concentration shows little interannual variability, the impacts on production and oxygen vary substantially according to whether a specific year is particularly dry or wet (Figure 8d and 8g). Specifically, in dry, low-flow years riverine DIN loading is reduced and the available DIN is assimilated in the oligohaline and upper mesohaline Bay, thus providing less DIN advection to the lower mesohaline Bay (Figure 9a). Because nitrogen is therefore more limiting in the middle Bay in dry years, the impact of additional DIN inputs to this portion of the Bay is stronger in such years. In the middle Bay, doubling atmospheric deposition has almost twice as great an impact on production in a dry year than a wet year (Figure 8d) and therefore twice as great an impact on bottom oxygen as well (Figure 8g). During the wet year, higher river flow carries more DIN to the middle Bay than in the dry year (Figure 9b), and results in the annual phytoplankton bloom and production maximum being located in more seaward regions of the Bay (Figure 9d; Hagy et al. 2005, Testa and Kemp 2014). Thus in the wet year, instead of the middle Bay being the most nutrient-limited region, the lower Bay becomes the most DIN-depleted. As a result, the location of maximum increase in primary production and decrease in bottom oxygen due to atmospheric depositions migrates farther downstream in wet years compared to dry years. Additionally, since phytoplankton in the lower Bay are always nitrogen limited, the larger atmospheric DIN deposition in wetter years (Table 1) results in the impact of atmospheric deposition in the lower Bay being greater in wet years than dry years for both productivity and oxygen (Figure 8d and 8g).

Biogeochemical processes and estuarine circulation together determine the interannual variability associated with impacts of coastal DIN inputs. As discussed above, in both dry and wet years, phytoplankton in the surface waters of the polyhaline Bay are always the most nitrogen-limited (Figure 9a and 9b). In this region, increases in DIN due to higher DIN concentrations on the shelf are similar in both years (Figure 8c), and increases in PP in the polyhaline Bay also show very little interannual variability (Figure 8f). On the contrary, the middle Bay is more nitrogen limited in dry years than wet years, and is thus more sensitive to coastal DIN inputs during dry years. Thus the increase in PP

and decrease in bottom DO in the middle Bay are larger in dry years than wet years (Figure 8f and 8i). Estuarine dynamics theory indicates that the exchange flow at the Bay mouth increases with river discharge following a  $2/3$  power law (Geyer 2010; Scully 2013). Thus, during high flow years, the enhanced circulation causes a larger increase in seaward flux of low-DIN waters exiting from the Chesapeake Bay at the surface, and a larger increase in landward DIN flux from the coastal ocean at depth in response to increased coastal DIN inputs (Table 7). In addition, the increased advection (+114%) of lower oxygen water from the shelf into the polyhaline Bay causes DIN inputs from the coastal ocean to result in almost doubled impacts in lower Bay bottom oxygen concentrations in wet years compared to dry years (Figure 8i).

#### **4.4 Spatial Variability of Bottom Oxygen Response to Atmospheric and Coastal DIN Inputs**

DIN inputs from the atmosphere, coastal ocean and rivers all impact summer hypoxia, but the locations of their largest contributions differ spatially throughout the Bay. Since over 90% of freshwater inputs are from the three major rivers (i.e. the Susquehanna, Potomac and James Rivers), riverine DIN inputs have the greatest impact on dissolved oxygen in the upper Bay and inside these largest tributaries (Figure 10a). On the contrary, atmospheric DIN deposition has the greatest impact on bottom oxygen in the shallow regions of the Bay closest to land (e.g. in the small tributaries and on the shoals) where atmospheric DIN is greatest (Schwede & Lear, 2014). In the model, only a small amount of riverine nitrogen enters the Bay from the east, leading to a minimal influence from rivers on the shallow eastern shoals and subsequently resulting in a larger relative impact of atmospheric nitrogen in these regions. Lastly, because the lower Bay is most exposed to the continental shelf waters, coastal DIN inputs have the greatest impact there. In the central portion of the Bay where summer hypoxia is most prevalent, all three sources of DIN have substantial impacts on bottom oxygen (Figure 10a), with the inputs of atmospheric and coastal nitrogen being nearly equally important (Table 5).

In the winter, DIN inputs from the continental shelf strongly influence bottom oxygen concentrations throughout the majority of the Bay (Figure 10b). This is partially a result of the fact that climatological DIN concentrations on the continental shelf peak in winter (Figure 2c). Additionally, enhanced estuarine circulation in the winter due to high

winter river discharge (Geyer 2010; Scully 2013) helps extend the impacts of coastal DIN farther upstream. However, although coastal nitrogen sources have a relatively strong impact on bottom oxygen concentrations in the winter (Figure 10b), the percent impact on bottom oxygen is very small (0.49%; Table 5), since oxygen concentrations in the winter are very high.

#### **4.5 Future Work**

Although the modified *ChesROMS*-ECB model applied in this study reproduces most physical and biogeochemical fields well (see Appendix B), the following future efforts may further improve the model's performance. First, the temporal variability of particulate organic nitrogen is not well captured, which is likely at least partially due to the fact that the model includes only one type of phytoplankton and zooplankton. Adding another phytoplankton species with a lower optimal temperature and a different carbon to chlorophyll ratio (Xiao & Friedrichs, 2014a,b) would likely improve model estimates of bottom particulate organic nitrogen and chlorophyll during the spring in the upper mesohaline Bay. Additionally, including phosphate limitation could improve the realism of the model simulations, since oceanic phosphorus and sediment phosphorus fluxes can play an important role in Chesapeake Bay nutrient cycling, especially in the upper Bay and spring/winter seasons when phosphorus can be more limiting than nitrogen (Kemp et al., 2005). Furthermore, incorporating a sediment-biogeochemical model could improve the estimates of oxygen and nutrients fluxes at seabed-water column interface, eventually isolating the impact on DO from sediment nutrient supply (Moriarty et al., 2017). Nudging to interannually varying DIN concentrations along the model open boundary will be important as more in situ data become available in the future.

Although in the current version of *ChesROMS*-ECB riverine inputs to the Bay are distributed to only the ten largest tributaries (Figure 1), current work is underway to improve the realism of the locations of these freshwater inputs. In the real world there are thousands of rivers and creeks exporting inorganic and organic materials to the Chesapeake Bay. Thus, increasing the number of locations where these inputs enter the model grid will make future model simulations more realistic. For example, the eastern mesohaline Bay is strongly influenced by heavy fertilizer application in eastern Maryland and Virginia, so nutrients coming from surface runoff could be substantial (Ator &

Denver, 2015). The addition of more localized terrestrial inputs to the model could potentially lower the importance of atmospheric DIN deposition in shallow near-shore regions. However, applying spatially higher-resolution atmospheric deposition products when they become available will be an important model improvement as well, and could potentially increase the impact of atmospheric inputs in near-shore regions where deposition is generally largest. Lastly, including tidal wetlands in *ChesROMS-ECB* could be important since Najjar et al. (2018) indicate that tidal wetlands play a crucial role in coastal biogeochemical cycling.

## 5. Summary and Conclusions

This study examines the relative impacts of two additional sources of DIN on Chesapeake Bay bottom oxygen concentrations: direct atmospheric DIN deposition and coastal DIN inputs at depth. Through the use of an extensively evaluated three-dimensional hydrodynamic-estuarine-carbon-biogeochemistry model (Feng et al., 2015; Irby et al., 2016; Irby et al., 2017), atmospheric and coastal DIN inputs are found to substantially impact Chesapeake Bay primary production and DO, especially in the summer (up to  $200 \text{ mg-C m}^{-2} \text{ d}^{-1}$  and  $0.3 \text{ mg L}^{-1}$ , respectively). Direct atmospheric DIN deposition causes nearly the same impact on hypoxia as the same gram for gram change in riverine DIN loading. During dry years, the impact resulting from atmospheric DIN input on primary production and bottom oxygen is greatest in the nutrient-limited mid-Bay. This greatest impact is farther downstream in wet years. The coastal ocean is another important source of DIN for the Bay and has a similar impact on summer hypoxia as direct atmospheric DIN deposition. In contrast, the impact on winter DO is much greater than that resulting from direct atmospheric DIN deposition. Spatially, the atmospheric DIN input has greatest impact on oxygen in the shallow near-shore regions of the Bay, while coastal DIN input has greatest impact in the lower Bay.

When studying Chesapeake Bay eutrophication and hypoxia, researchers typically focus on riverine DIN loading, while often neglecting other potential DIN sources such as direct atmospheric DIN deposition and deep DIN inputs from the coastal ocean (Feng et al., 2015; Li et al., 2016). In this research, careful integration of DIN from all three of these different sources produced a more realistic and reliable simulation of

biogeochemical dynamics in the Chesapeake Bay, and quantified the considerable impacts that direct atmospheric DIN deposition and coastal DIN inputs have on primary production and hypoxia. Considering long-term trends in atmospheric DIN deposition is critical for demonstrating the positive estuarine impacts resulting from the success that has been made in reducing airborne pollutants (Paerl, 1997). Finally, future sea level rise, which has been predicted to increase estuarine circulation (Irby et al., 2017), also needs to be taken into account as it will likely increase the impact of coastal nitrogen fluxes on future hypoxia in Chesapeake Bay.

## **Acknowledgments:**

This work has been supported by the NASA Interdisciplinary Science Program (NNX14AF93G) and by the National Science Foundation (OCE-1259187). This work was performed using High Performance Computing facilities at the College of William & Mary, which were provided by contributions from the National Science Foundation, the Commonwealth of Virginia Equipment Trust Fund and the Office of Naval Research. I would like to thank Kyle Hinson and the Chesapeake Bay Program Watershed Modeling group for providing the riverine and atmospheric input files.

**Table 1.** Inputs of DIN to the Chesapeake Bay from Direct Atmospheric Deposition and Riverine Loading

	Average	2002 Dry <sup>#</sup>	2003 Wet	2004 Wet	2005 Normal
Atmospheric DIN inputs (Gg-N y <sup>-1</sup> )	8.0	7.7	9.3	7.2	7.9
Riverine DIN inputs (Gg-N y <sup>-1</sup> )	91	73	120	88	83
$\Delta =$ 100*Atmospheric/Riverine (%)	8.8	10.5	7.7	8.2	9.5

<sup>#</sup>Dry and wet years are based on annual riverine discharge to the Chesapeake Bay

**Table 2.** List of DIN Input Sensitivity Experiments

Simulations	Atmospheric DIN inputs	Coastal DIN inputs	Riverine DIN inputs
Reference run	Realistic <sup>*</sup>	Realistic	Realistic
Atmospheric deposition runs (AtmN)	None <sup>&amp;</sup>	Realistic	Realistic
	Double <sup>#</sup>	Realistic	Realistic
Coastal ocean runs (CoastalN)	Realistic	None <sup>&amp;</sup>	Realistic
	Realistic	Double	Realistic
River forcing runs ( $\Delta$ RiverN)	Realistic	Realistic	$\Delta\downarrow^{\dagger}$ in DIN
	Realistic	Realistic	$\Delta\uparrow$ in DIN

<sup>\*</sup>“Realistic” refers to realistic inputs (nudging at open boundary, total riverine DIN inputs, or total atmospheric DIN deposition)

<sup>†</sup>  $\Delta\downarrow$  denotes that river inputs are reduced by the amount of atmospheric DIN deposition, i.e. ~9%.

<sup>&</sup> “None” denotes no inputs: nudging to zero DIN concentration at the open boundary or no atmospheric deposition

<sup>#</sup> “Double” denotes doubled atmospheric deposition, or nudging to doubled DIN concentrations at the open boundary.



**Table 3.** Absolute and Percent Difference in Depth-averaged DIN Between the Three Sensitivity Experiments (Table 1) and the Reference Run

Seasons	Absolute difference (mmol-N m <sup>-3</sup> )*					Percent difference (%)*				
	Annual	Spring	Summer	Fall	Winter	Annual	Spring	Summer	Fall	Winter
AtmN	1.4	1.6	1.0	1.3	1.8	4.7	4.8	4.2	4.8	4.9
ΔRiverN	2.0	2.8	1.6	1.4	2.4	6.7	8.4	6.6	5.2	6.5
CoastalN	0.8	1.2	0.6	0.5	1.0	2.8	3.7	2.5	1.9	2.8

*Note.* Numbers are computed along the mainstem transect between stations CB3.3C and CB6.2 (Figure 1), where hypoxia is the most prevalent.

\*In each case results are shown for the average of the two sensitivity experiments (DIN increase and DIN decrease tests).

For example, the absolute and percent difference in depth-averaged DIN resulting from the AtmN experiment are calculated as:

$$\begin{aligned} \Delta DIN_{+AtmN} &= abs(DIN_{reference} - DIN_{+AtmN}) \\ \Delta DIN_{-AtmN} &= abs(DIN_{reference} - DIN_{-AtmN}) \\ Absolute \Delta DIN_{AtmN} &= \frac{\Delta DIN_{+AtmN} + \Delta DIN_{-AtmN}}{2} \\ Percent \Delta DIN_{AtmN} &= \frac{Absolute \Delta DIN_{AtmN}}{DIN_{reference}} \times 100\% \end{aligned}$$

**Table 4.** Absolute and Percent Difference in Depth-integrated PP Between the Three Sensitivity Experiments (Table 1) and the Reference Run

Seasons	Absolute difference (mg-C m <sup>-2</sup> d <sup>-1</sup> )*					Percent difference (%)*				
	Annual	Spring	Summer	Fall	Winter	Annual	Spring	Summer	Fall	Winter
AtmN	24	16	62	16	2.7	2.2	1.5	2.6	2.1	1.7
ΔRiverN	29	20	81	13	2.2	2.6	1.9	3.3	1.7	1.3
CoastalN	10	6.4	28	6.7	0.8	0.9	0.6	1.1	0.9	0.5

*Note.* Numbers are computed along the mainstem transect between stations CB3.3C and CB6.2 (Figure 1), where hypoxia is most prevalent.

\*In each case results are shown for the average of the two sensitivity experiments (DIN increase and DIN decrease tests)

**Table 5.** Absolute and Percent Difference in Bottom DO Between the Three Sensitivity Experiments (Table 1) and the Reference Run

Seasons	Absolute difference (mg L <sup>-1</sup> )*					Percent difference (%)*				
	Annual	Spring	Summer	Fall	Winter	Annual	Spring	Summer	Fall	Winter
AtmN	0.09	0.09	0.17	0.09	0.03	1.4	1.1	8.6	1.5	0.29
ΔRiverN	0.08	0.08	0.18	0.06	0.01	1.3	1.0	9.2	1.0	0.15
CoastalN	0.10	0.12	0.16	0.07	0.05	1.6	1.6	8.5	1.3	0.49

*Note.* Numbers are computed along the mainstem transect between stations CB3.3C and CB6.2 (Figure 1), where hypoxia is most prevalent.

\*In each case results are shown for the average of the two sensitivity experiments (DIN increase and DIN decrease tests)

**Table 6.** Absolute and Percent Difference in Cumulative Hypoxic Volumes Between the Three Sensitivity Experiments (Table 1) and the Reference Run

DO level (mg L <sup>-1</sup> )	Absolute difference (km <sup>3</sup> d) <sup>&amp;</sup>				Percent difference (%) <sup>&amp;</sup>			
	<5 <sup>*</sup>	<2	<1	<0.2	<5	<2	<1	<0.2
AtmN	94	48	31	11	5.6	11	16	23
ΔRiverN	93	51	34	13	5.6	12	17	26
CoastalN	95	43	27	9	5.7	10	14	19

<sup>\*</sup>The differences in hypoxic volume are calculated with different threshold: DO < 5/2/1/0.2 mg L<sup>-1</sup>.

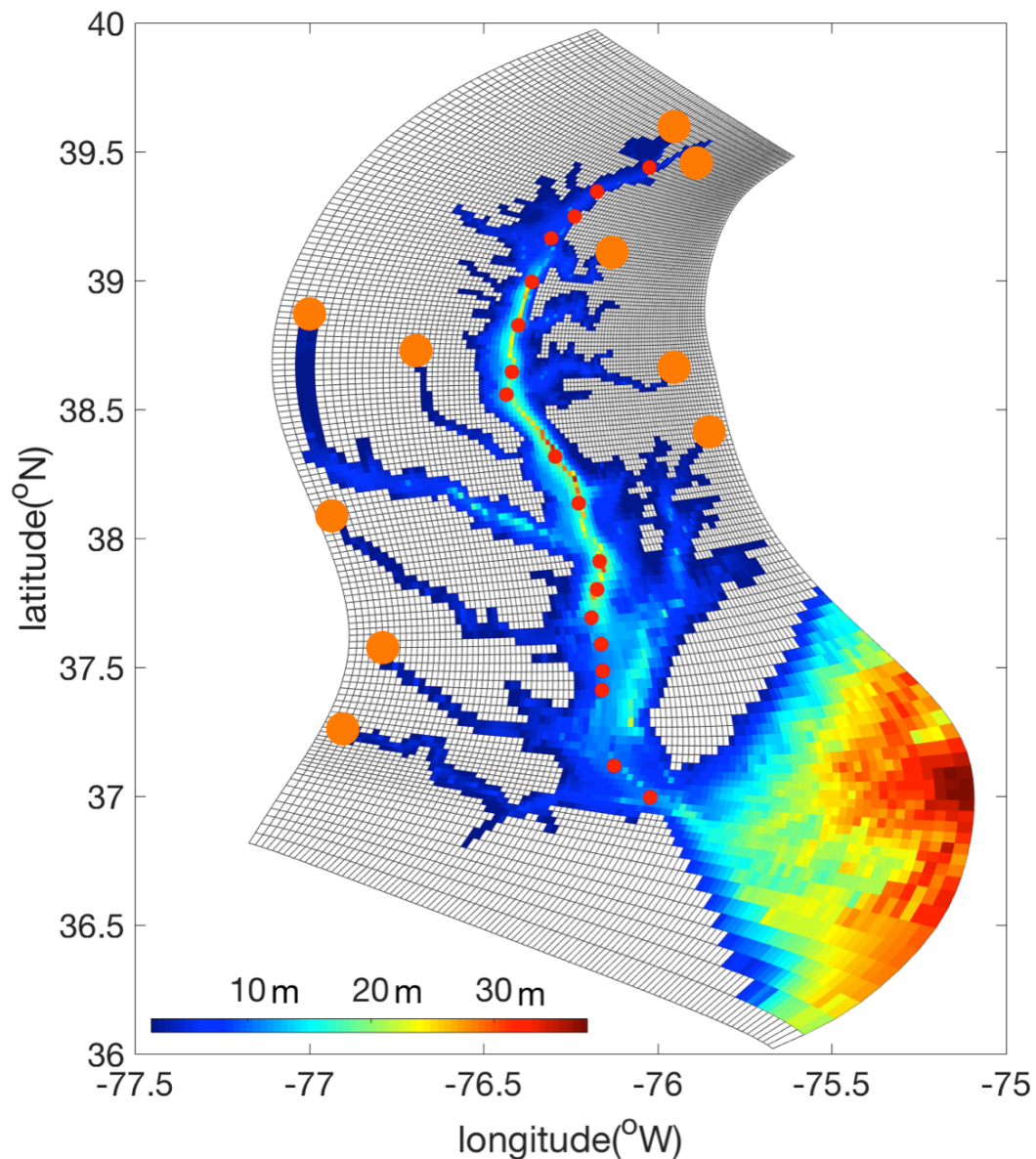
<sup>&</sup>In each case results are shown for the average of the two sensitivity experiments (DIN increase and DIN decrease tests)

**Table 7.** Reference run annual DIN fluxes and the changes in DIN fluxes at the mouth of the Bay due to coastal DIN input

	DIN flux	Average	2002 Dry	2003 Wet	2004 Wet	2005 Normal
Reference run DIN flux (Gg-N yr <sup>-1</sup> )	Seaward flux at surface	43	13	65	56	37
	Landward flux at depth	19	12	24	22	16
	Net flux*	24	1	41	34	21
Changes in DIN flux due to CoastalN (Gg-N yr <sup>-1</sup> )	ΔSeaward flux	4.4	2.3	5.9	5.4	4.0
	ΔLandward flux	5.3	4.0	6.6	6.1	4.6
	ΔNet flux**	-0.9	-1.7	-0.7	-0.7	-0.6

\*Positive values imply the net flux is directed seaward

\*\*Negative values imply the net seaward flux is reduced





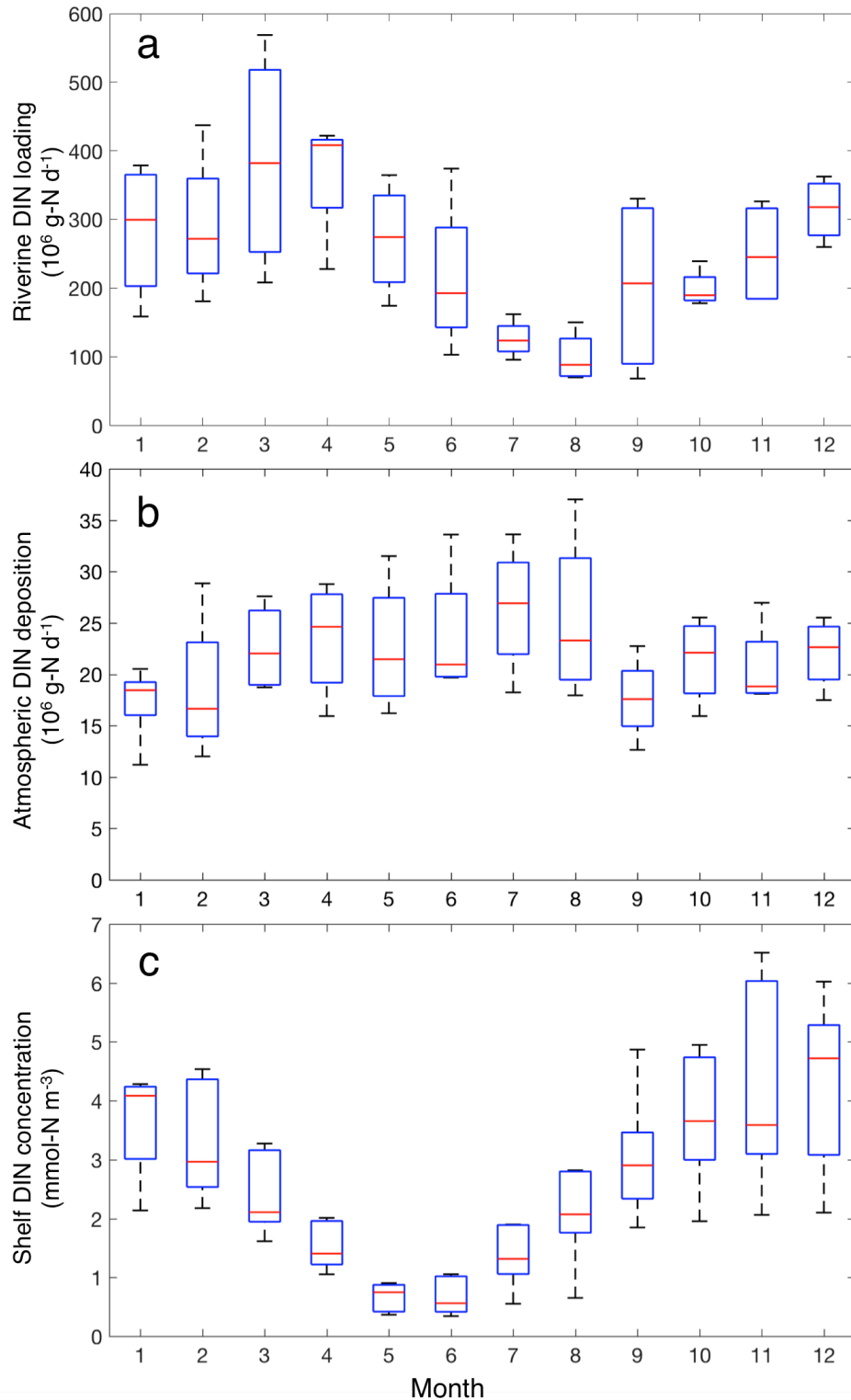


**Figure 1.** The Chesapeake Bay bathymetry, horizontal coordinate system (light grey grid cells) of *ChesROMS-ECB*, and stations (red dots) along the mainstream of the Bay. (Stations from upper to lower Bay are as follows: CB2.1, CB2.2, CB3.1, CB3.2, CB3.3C, CB4.1C, CB4.2C, CB4.3C, CB5.1, CB5.2, CB5.3, CB5.4, CB5.5, CB6.1, CB6.2, CB6.3, CB7.3, and CB7.4.) Orange circles denote the ten locations of watershed inputs, representing the largest rivers entering the Bay.

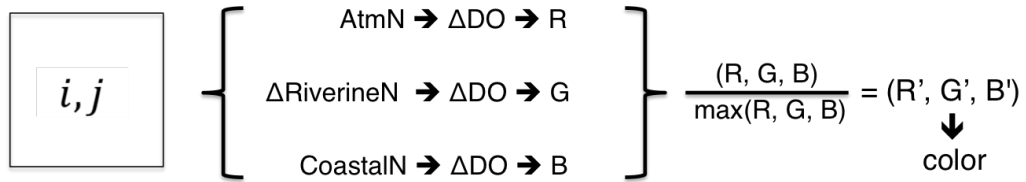


**Figure 2.** Average seasonality of DIN inputs to *ChesROMS-ECB*: (a) riverine DIN loading, (b) direct atmospheric DIN deposition, (c) depth averaged open boundary DIN concentrations (interpolation from Melrose et al. (2015) dataset). Red lines show median values, the bottom and top edges of the blue boxes indicate the 25th and 75th percentiles, respectively. The whiskers extend to the most extreme data points.



- e.g.  $R=3, G=0, B=0 \rightarrow \text{color} = (1, 0, 0) \rightarrow$  
- e.g.  $R=0, G=4, B=0 \rightarrow \text{color} = (0, 1, 0) \rightarrow$  
- e.g.  $R=0, G=0, B=2 \rightarrow \text{color} = (0, 0, 1) \rightarrow$  
- e.g.  $R=2, G=2, B=2 \rightarrow \text{color} = (1, 1, 1) \rightarrow$  

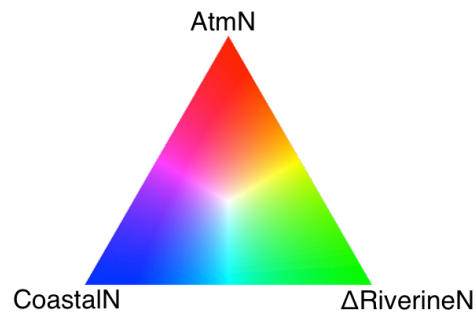


**Figure 3.** Schematic of the method calculating the relative impacts on bottom DO from the three sensitivity experiments (Table 1) in each grid cell (i,j).



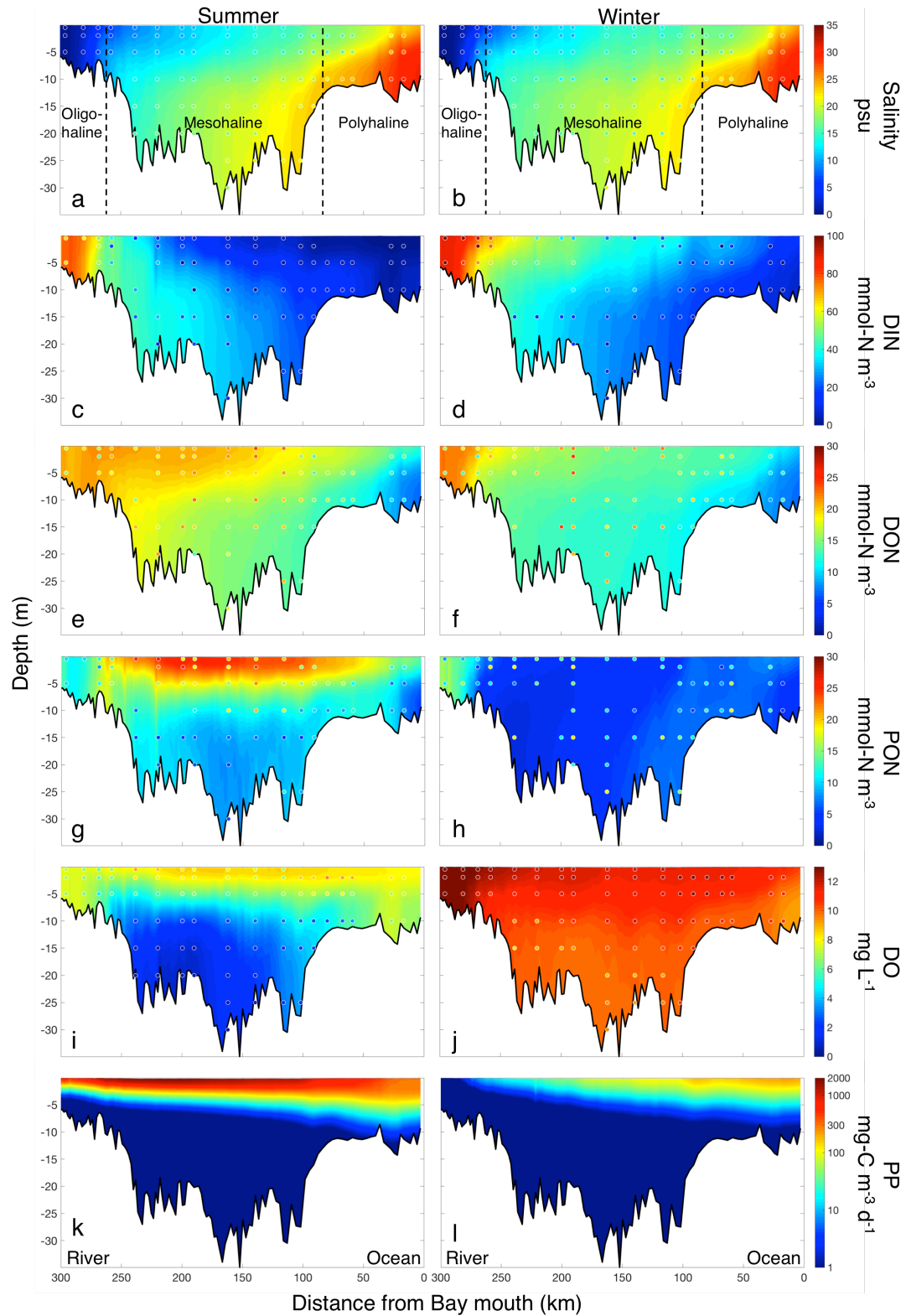


**Figure 4.** Four-year (2002-2005) averages of: (a-b) salinity, (c-d) DIN, (e-f) DON, (g-h) PON, (i-j) DO, (k-l) primary production (PP) shown for the summer (a,c,e,g,i,k) and winter (b,d,f,h,j,l). Colored contours represent model results; circles represent CBP observations.

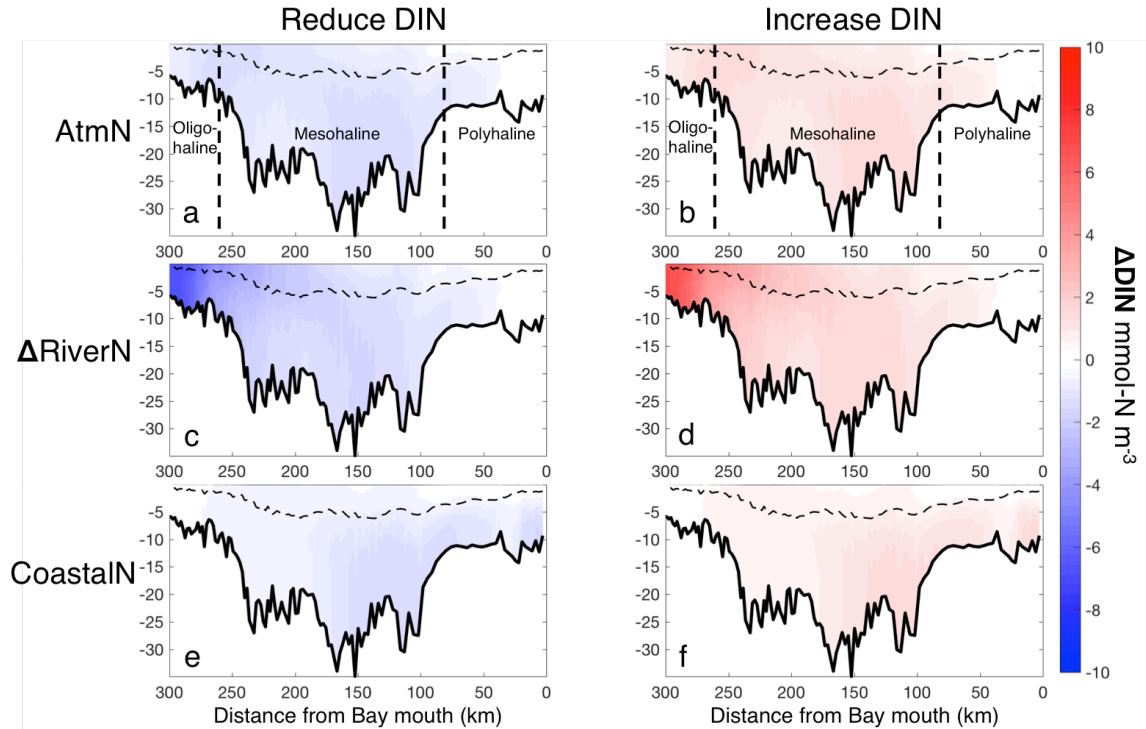


**Figure 5.** Four-year (2002-2005) averages of changes in DIN in the summer resulting from: (a,b) AtmN sensitivity experiments, (c,d)  $\Delta$ RiverN sensitivity experiments, (e,f) CoastalN sensitivity experiments; (a,c,e) denotes DIN reduction, (b,d,f) denotes DIN increase. Dashed lines are four-year (2002-2005) averaged summertime pycnocline (defined as in Irby et al. (2016)).

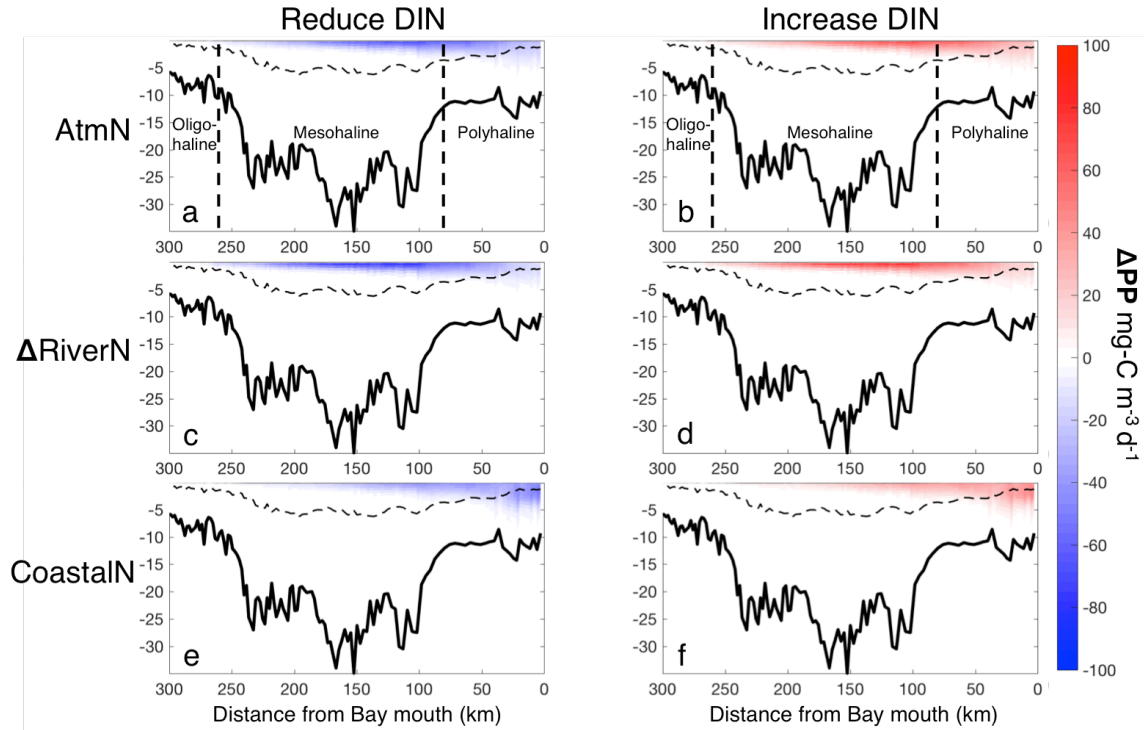


**Figure 6.** Four-year (2002-2005) averages of changes in primary production (PP) in the summer resulting from: (a,b) AtmN sensitivity experiments, (c,d)  $\Delta$ RiverN sensitivity experiments, (e,f) CoastalN sensitivity experiments; (a,c,e) denotes DIN reduction, (b,d,f) denotes DIN increase. Dashed lines are four-year (2002-2005) averaged summertime pycnocline.

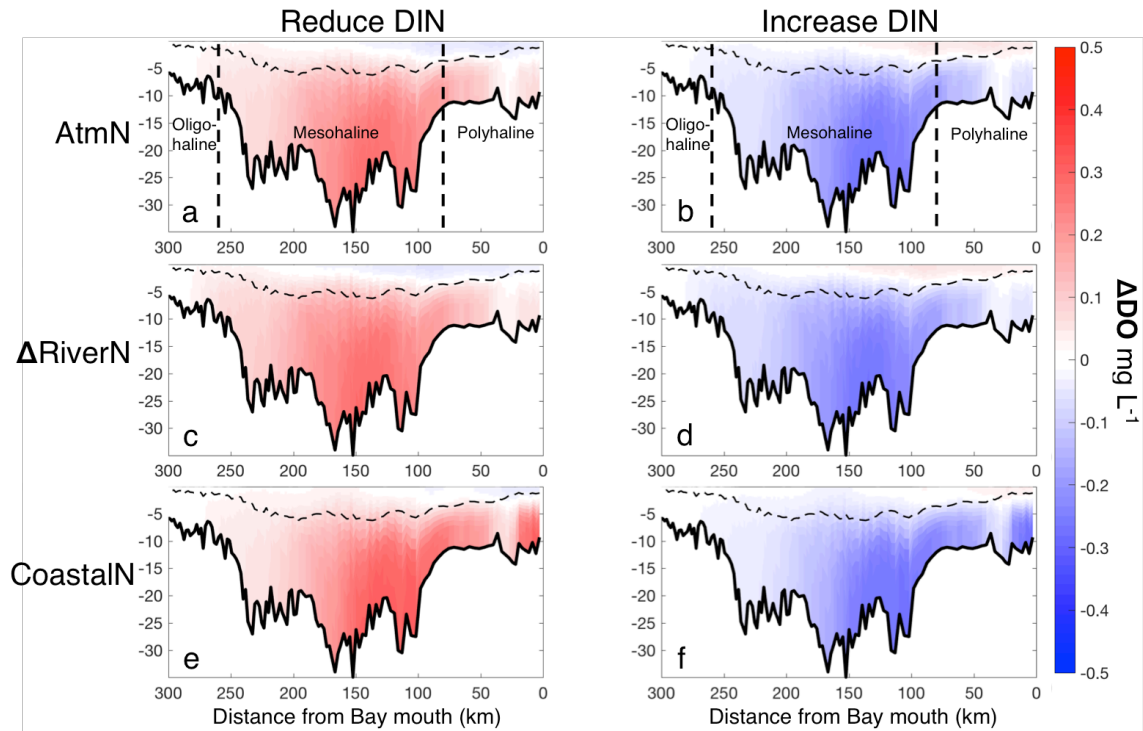


**Figure 7.** Four-year (2002-2005) averages of changes in DO in the summer resulting from: (a,b) AtmN sensitivity experiments, (c,d)  $\Delta$ RiverN sensitivity experiments, (e,f) CoastalN sensitivity experiments; (a,c,e) denotes DIN reduction, (b,d,f) denotes DIN increase. Dashed lines are four-year (2002-2005) averaged summertime pycnocline.

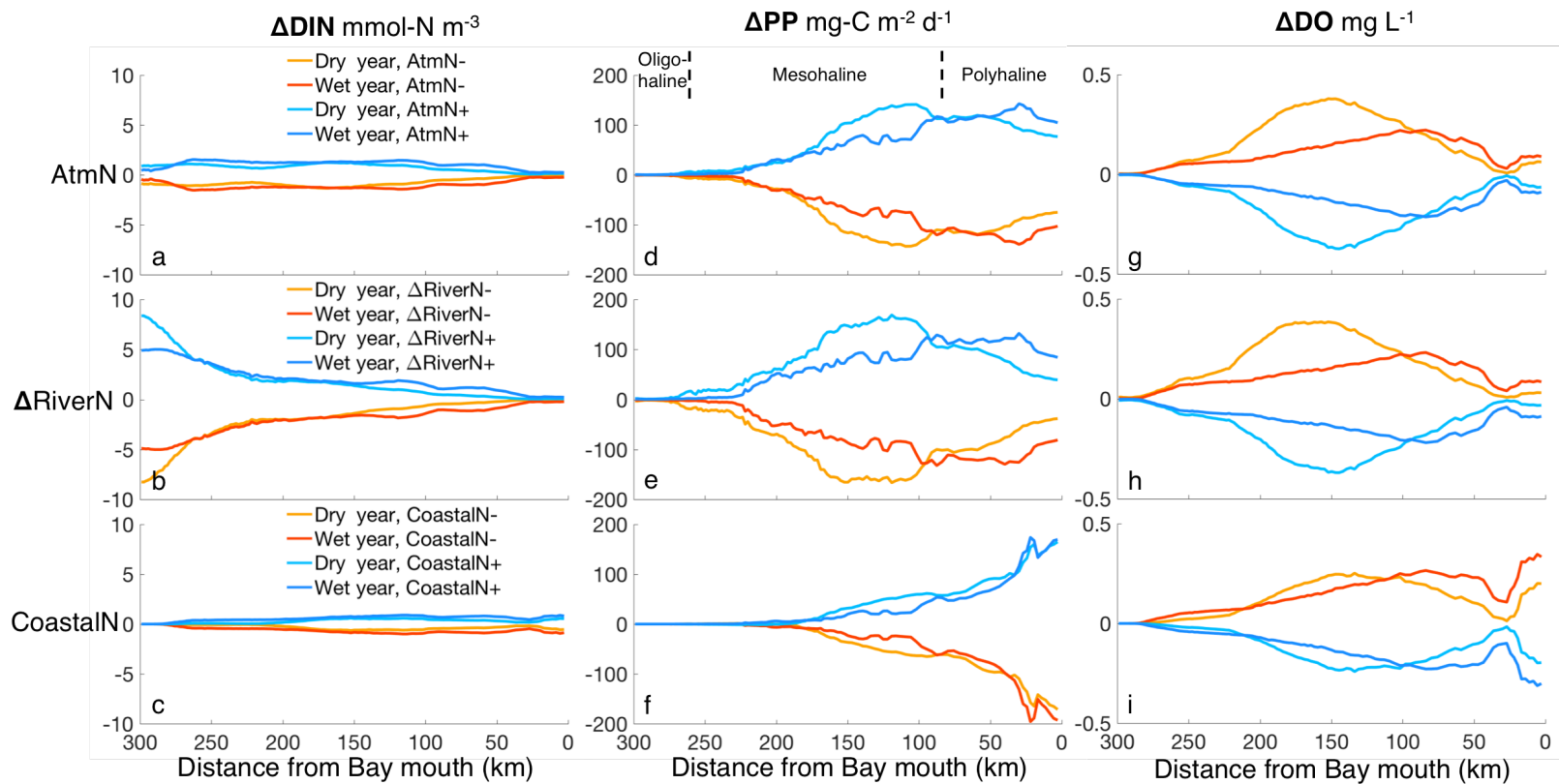


**Figure 8.** Impacts of three sensitivity experiments (Table 1) on: (a-c) summer depth-averaged DIN, (d-f) depth-integrated primary production, (g-i) bottom DO in the driest year considered (2002) and the wettest year (2003); (a,d,g) AtmN sensitivity experiments, (b,e,h)  $\Delta$ RiverN sensitivity experiments, (c,f,i) CoastalN sensitivity experiments.

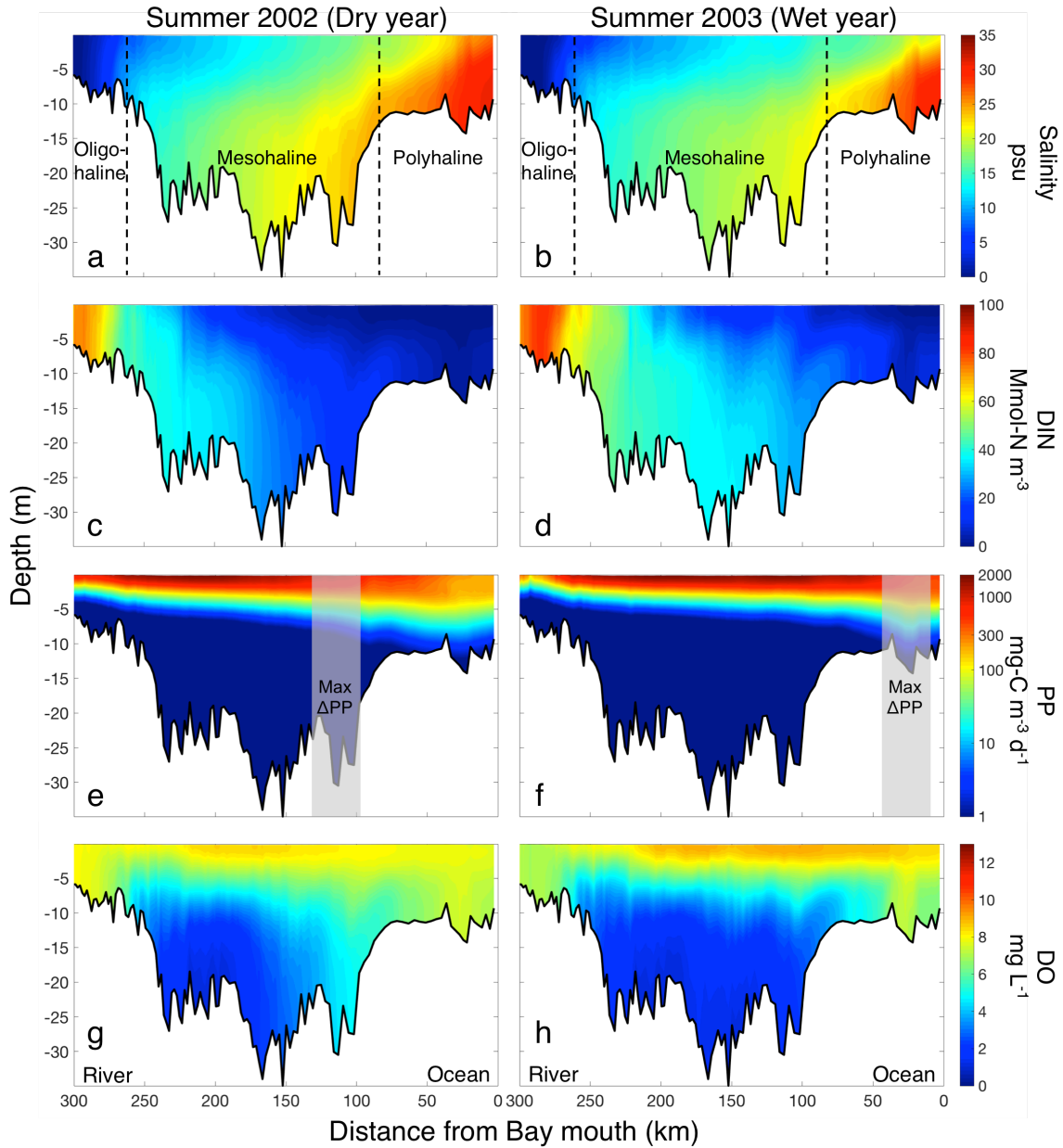


**Figure 9.** Model results of (a,b) salinity, (c,d) DIN, (e,f) primary production, and (g,h) DO along the mainstem of the Chesapeake Bay; (a,c,e,g) denotes summer 2002 (a dry year), and (b,d,f,h) denotes summer 2003 (a wet year). The shading areas represent the maximum changes in primary production resulting from atmospheric DIN deposition.

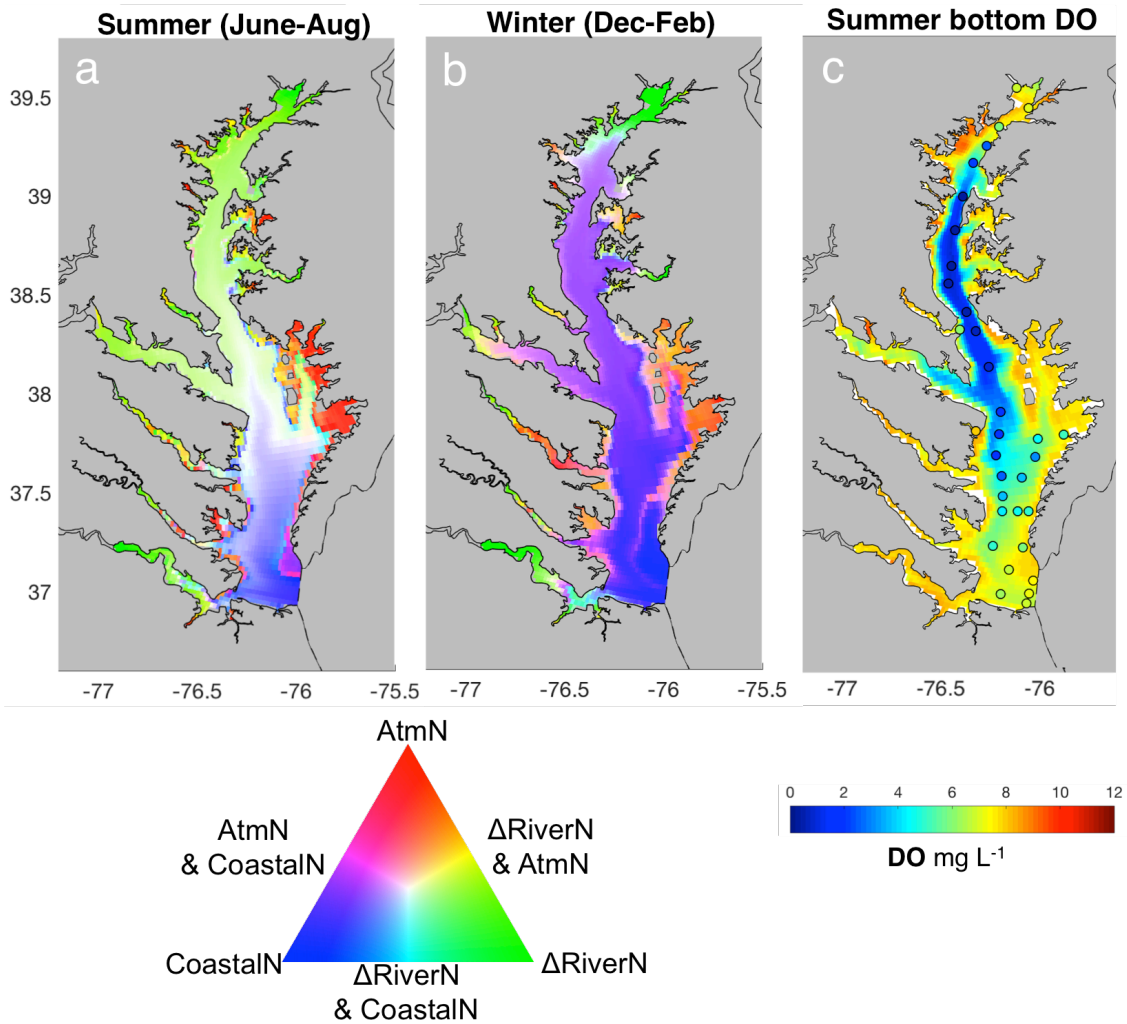


**Figure 10.** Relative impacts on bottom DO resulting from the three sensitivity experiments (Table 1) during: (a) summer, (b) winter; (c) summertime bottom DO averaged over 2002-2005 (circles represent CBP observations).

## Appendix A Modified ChesROMS-ECB Parameters

Model parameters modified from those used in Feng et al. (2015) are listed below in Table A1.

## Appendix B ChesROMS-ECB Skill Assessment

Quantitative metrics are applied to evaluate how well the model reproduces the available data at 18 stations in the mainstem of the Chesapeake Bay (Table B1). Model simulations and observations at the same times and locations are compared to achieve point-to-point comparisons. First, the standard deviation of the model predictions ( $\sigma_p$ ) and CBP Water Quality Database observations ( $\sigma_o$ ), as well as normalized standard deviation of the model estimates ( $\sigma_r$ ) are calculated:

$$\sigma_o = \sqrt{\frac{\sum_{i=1}^n (O_i - \bar{O})^2}{n}}$$
$$\sigma_p = \sqrt{\frac{\sum_{i=1}^n (P_i - \bar{P})^2}{n}}$$
$$\sigma_r = \frac{\sigma_p}{\sigma_o}$$

where  $O_i$  is the observation at time  $t_i$  of a station at a specific depth, and  $P_i$  is the corresponding model prediction at time  $t_i$  with the same spatial location as the observation. The mean of the in situ data and model estimates are represented by  $\bar{O}$  and  $\bar{P}$  respectively. Here  $n$  is the total number of observations of a variable.

*Bias* (the average error) between observations and predictions, unbiased root-mean-square difference (*ubRMSD*), and total root-mean-square difference (*RMSD*) are three additional important skill statistics for assessment. The total *RMSD* can be calculated from *bias* and *ubRMSD*:

$$bias = \frac{\sum_{i=1}^n (P_i - O_i)}{n} = \bar{P} - \bar{O}$$
$$RMSD = \sqrt{\frac{\sum_{i=1}^n (P_i - O_i)^2}{n}}$$



$$ubRMSD = \sqrt{\frac{\sum_{i=1}^n [(P_i - \bar{P}) - (O_i - \bar{O})]^2}{n}}$$

$$Bias^2 + ubRMSD^2 = RMSD^2$$

These skill assessment metrics (Table B2) were visualized using target diagrams (Hofmann et al., 2008; Jolliff et al., 2009). Target diagrams show *RMSD*, *ubRMSD*, and *bias* in a Cartesian coordinate system (Figure B1). An additional metric, the sign of the difference between the standard deviation of the model estimates and that of the observations, is visualized by placing the uRMSD values on the positive or negative x-axis, respectively. The model skill metrics are illustrated in regards to spatial variability (Figure B1a), temporal variability (Figure B1b) and spatial-temporal variability (Figure B1c). Temperature and DO fields are well reproduced in terms of both spatial and temporal variability. The spatial variability skill for salinity, DIN, DON and PON is higher than that of the temporal variability, especially for salinity. Combined spatial and temporal analyses indicate that temperature, salinity, DO and DIN are well captured by the model. Additionally, the bias between modeled DON/PON and observations are very small, suggesting that the model simulates the averaged DON/PON fields well, but can be improved in light of temporal variability in the future.

In addition to the quantitative evaluations, the model results are also evaluated qualitatively for four individual regions of the Bay: the oligohaline (A), the upper mesohaline (B), the lower mesohaline (C) and the polyhaline (D). (See Table B1 for specific definitions). For surface and bottom temperature, salinity and DO, the model results agree well with monthly observations throughout the full simulation, although modeled bottom DO is  $\sim 2 \text{ mg L}^{-1}$  higher in the spring in region B (Figure B2-B4). DIN in the summer is relatively well captured by the model in all four regions, although the model overestimates surface and bottom DIN in the winter-spring seasons (Figure B5). For the DON model-data comparison, although modeled DON shows more seasonal variability than the in situ data, the average of model results and observations are very consistent throughout the four years studied (Figure B6). Modeled surface PON agrees with monthly in situ data relatively well in region C and D, but underestimates PON field in region B in the winter-spring. The model, especially in region B, does not capture the spring peak in bottom PON, but performs relatively well in region D (Figure B7).

**Table A1.** Modified Biogeochemical Parameters from Feng et al. (2015)

Symbol	Description	Feng et al. (2015) Value	New Value	Units
$g_{max}$	Zooplankton maximum growth rate	0.3	$0.05 * e^{0.0742 * T}$	$d^{-1}$
$TSS$	Total suspended solids	$ISS + \eta_{C:N}^* \frac{P + Z + D_S + D_L}{1000} \times 12$	$ISS + 4 + 2.9 \times \eta_{C:N} \frac{P + Z + D_S + D_L}{1000} \times 12$	$mg L^{-1}$
$K_D$	Light attenuation	$1.4 + 0.063[TSS] - 0.057S$ If $1.4 + 0.063[TSS] - 0.057S < 0$ , then $0.04 + 0.02486[Chl] +$ $0.003786\{0, 6.625 ([DON]_{SL} + [DON]_{RF}) - 70.819\}_{max}$	$1.4 + 0.063[TSS] - 0.057S$ If $1.4 + 0.063[TSS] - 0.057S < 0.6$ , then 0.6	$m^{-1}$
$r_{D_L}$	Remineralization of large detritus	0.2	$0.05 * e^{0.0742 * T}$	$d^{-1}$
$r_{D_S}$	Remineralization of small detritus	0.2	$0.05 * e^{0.0742 * T}$	$d^{-1}$
$\kappa_{[DON]_{SL}}$	Temperature dependency remineralization of semi-labile DON	0.07	0.0742	$(^{\circ}C)^{-1}$
$\mu_0$	Phytoplankton growth rate	2.15	If $T < 20$ , Then 2.15 Else, $1.81 + e^{0.16 * T - 4.28}$	$d^{-1}$

\*  $\eta_{C:N}$  denotes Phytoplankton carbon:nitrogen ratio, which equals 106/16 mol C/mol N (Feng et al., 2015).

**Table B1.** List of Stations for Model-data Comparison

#	Station name	Latitude (°N)	Longitude (°W)	Station depth (m)	ChesROMS-ECB depth (m)	Region
1	CB1.1	39.54794	-76.08481	6.1	2.4	A = Oligohaline <sup>&amp;</sup>
2	CB2.1*	39.44149	-76.02599	6.3	4.4	A
3	CB2.2*	39.34873	-76.17579	12.4	7.2	A
4	CB3.1*	39.24950	-76.24050	13.0	4.9	A
5	CB3.2*	39.16369	-76.30631	12.1	8.7	B = Upper Mesohaline
6	CB3.3C*	38.99596	-76.35967	24.3	19.4	B
7	CB4.1C*	38.82593	-76.39945	32.2	18.1	B
8	CB4.2C*	38.64618	-76.42127	27.2	18.8	B
9	CB4.3C*	38.55505	-76.42794	26.9	18.9	B
10	CB4.4	38.41457	-76.34565	30.3	22.0	B
11	CB5.1*	38.31870	-76.29215	34.1	28.4	C = Lower Mesohaline
12	CB5.2*	38.13705	-76.22787	30.6	26.1	C
13	CB5.3*	37.91011	-76.17137	26.9	25.8	C
14	CB5.4*	37.80013	-76.17466	31.1	20.3	C
15	CB5.5*	37.69180	-76.18967	17.0	16.3	C
16	CB6.1*	37.58847	-76.16216	12.5	12.3	D = Polyhaline
17	CB6.2*	37.48680	-76.15633	10.5	11.0	D
18	CB6.3*	37.41153	-76.15966	11.3	11.0	D
19	CB6.4	37.23653	-76.20799	10.2	9.6	D
20	CB7.1	37.68346	-75.98966	20.9	12.3	D
21	CB7.2	37.41153	-76.07966	20.2	14.6	D
22	CB7.3*	37.11681	-76.12521	13.6	11.4	D
23	CB7.4*	36.99570	-76.02048	14.2	11.0	D

\*Stations marked are along the Chesapeake Bay mainstem (Figure 1).

<sup>&</sup>Oligohaline is defined as surface salinity < 5psu, mesohaline is defined as surface salinity between 5-15psu, and polyhaline is defined as surface salinity > 15 psu.

**Table B2.** Model Skill Metrics Calculated with Spatial and Temporal Variability for Physical and Biogeochemical Fields

	meanM	meanO	stdM	stdO	Bias	ubRMSD	RMSD
Water temperature (°C)	15.35	14.93	8.29	8.39	0.43	1.42	1.48
Salinity (psu)	16.55	15.10	6.14	6.29	1.45	2.25	2.67
DO (mg L <sup>-1</sup> )	8.06	7.80	2.85	3.51	0.25	1.46	1.49
DIN (mmol-N m <sup>-3</sup> )	30.02	22.21	23.15	27.30	7.80	14.28	16.27
DON (mmol-N m <sup>-3</sup> )	15.68	17.20	4.03	4.24	-1.52	5.28	5.49
PON (mmol-N m <sup>-3</sup> )	11.35	11.56	6.08	5.48	-0.22	6.94	6.94

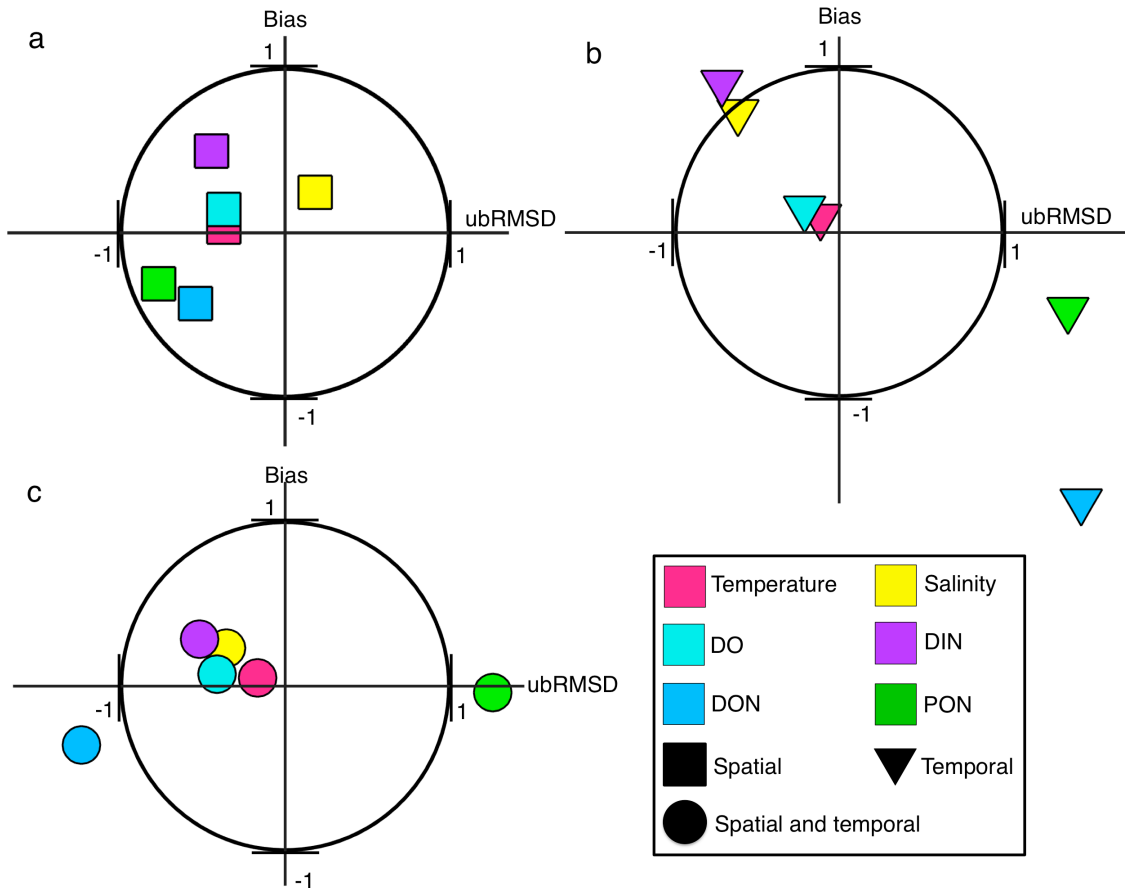


**Figure B1.** Target diagram illustrating model skill for physical and biogeochemical fields: (a) spatial variability (by comparing the four-year averaged model results and in situ data at the same stations and depths); (b) temporal variability (by comparing the model results and in situ data averaged over depth and 18 stations along mainstem); (c) spatial and temporal variability (this is point-to-point calculation by comparing monthly averaged model results and in situ data at the same depth, station and month). The x and y-axis represent unbiased root-mean-square-difference (ubRMSD) and bias, respectively, and the solid circles denote RMSD. All statistics are normalized by the standard derivation of observations.

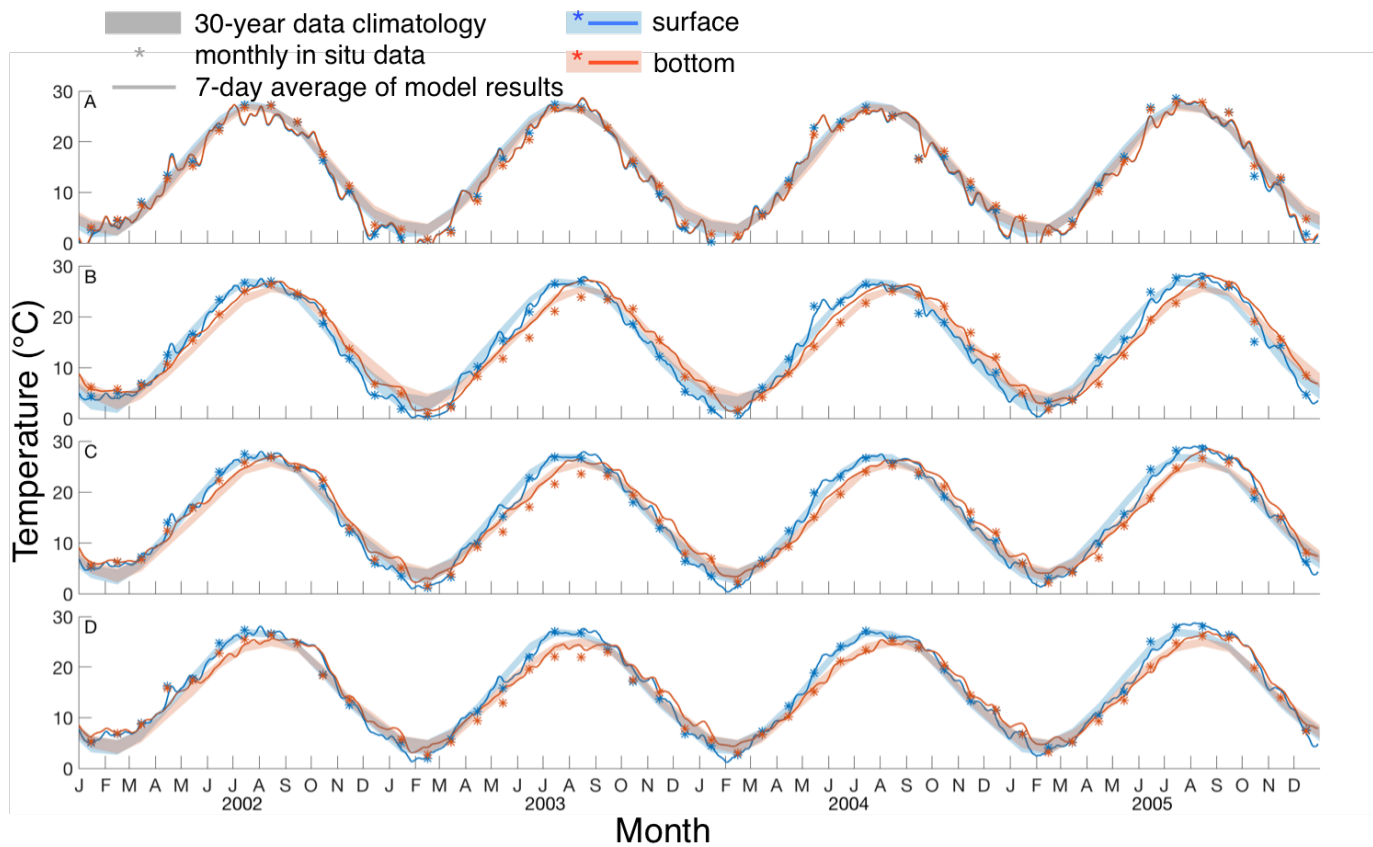


**Figure B2.** Model estimates (lines) and data (stars) showing spatially averaged temperature for 2002-2005 in the four regions (Table B1). Blue and red denotes surface and bottom, respectively. Shading represents the 30-year (1985-2014) data climatology, with the upper and lower boundaries of the shading representing the 75<sup>th</sup> and 25<sup>th</sup> percentiles of the climatology.

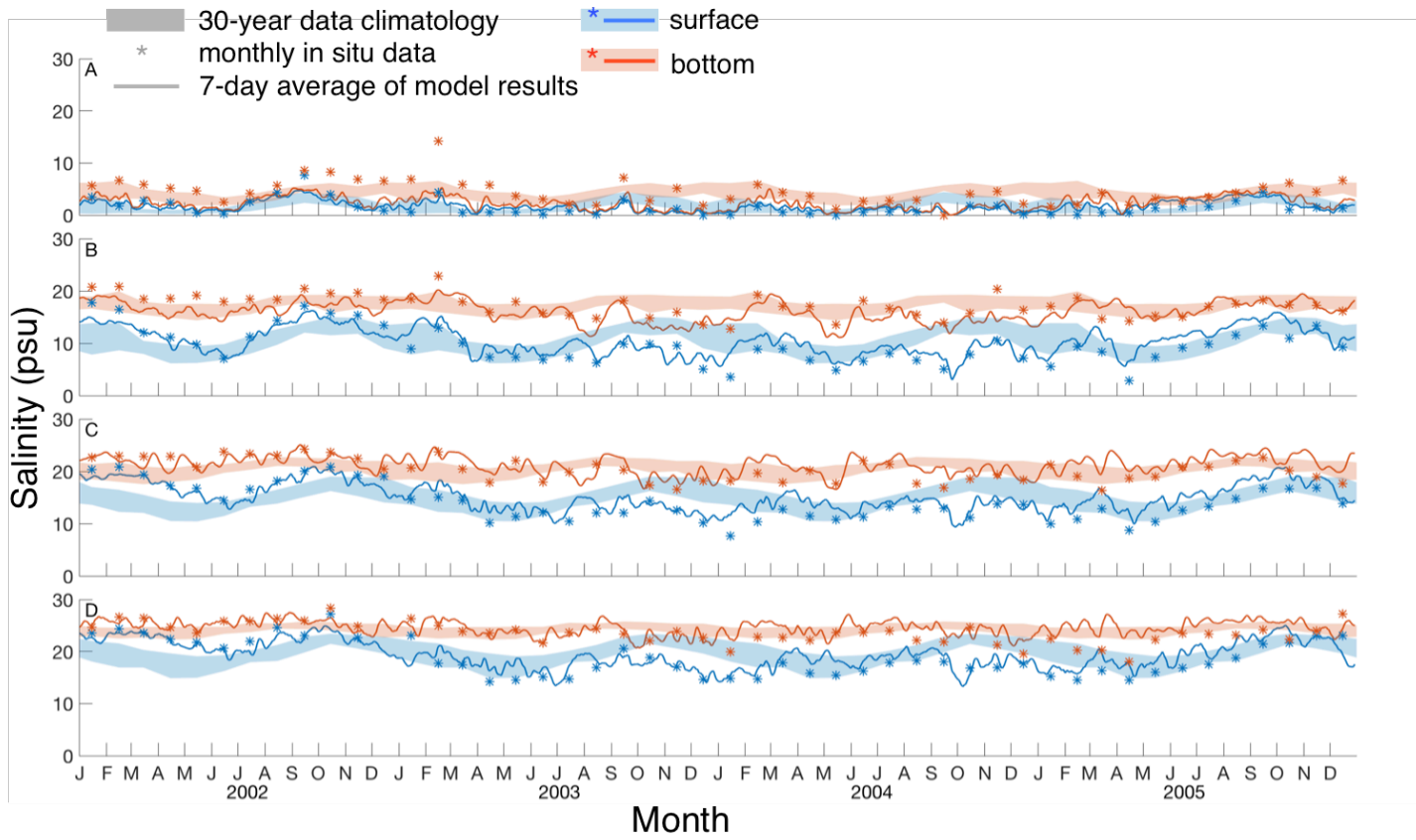


**Figure B3.** As in Figure B2, but for salinity.

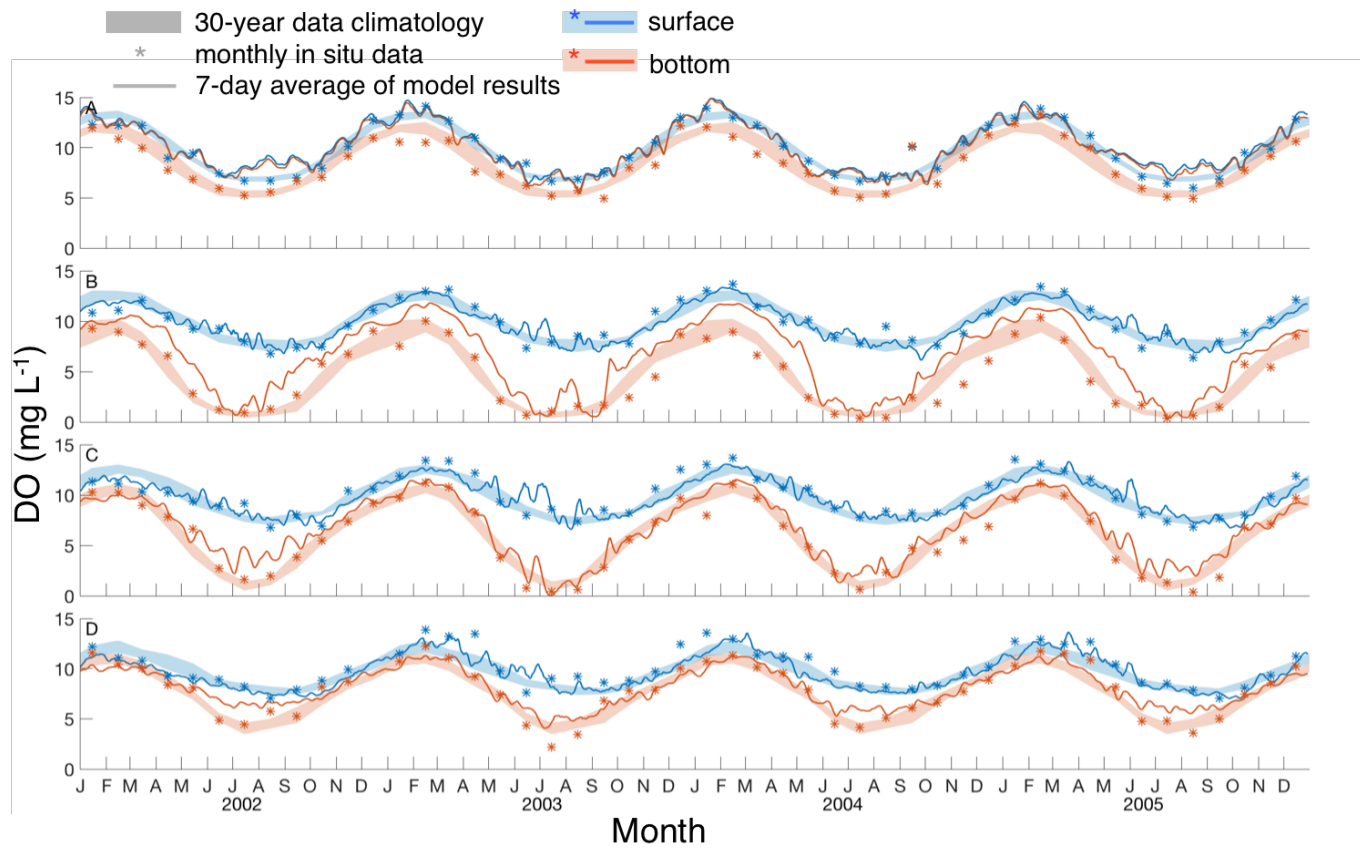


**Figure B4.** As in Figure B2, but for dissolved oxygen.



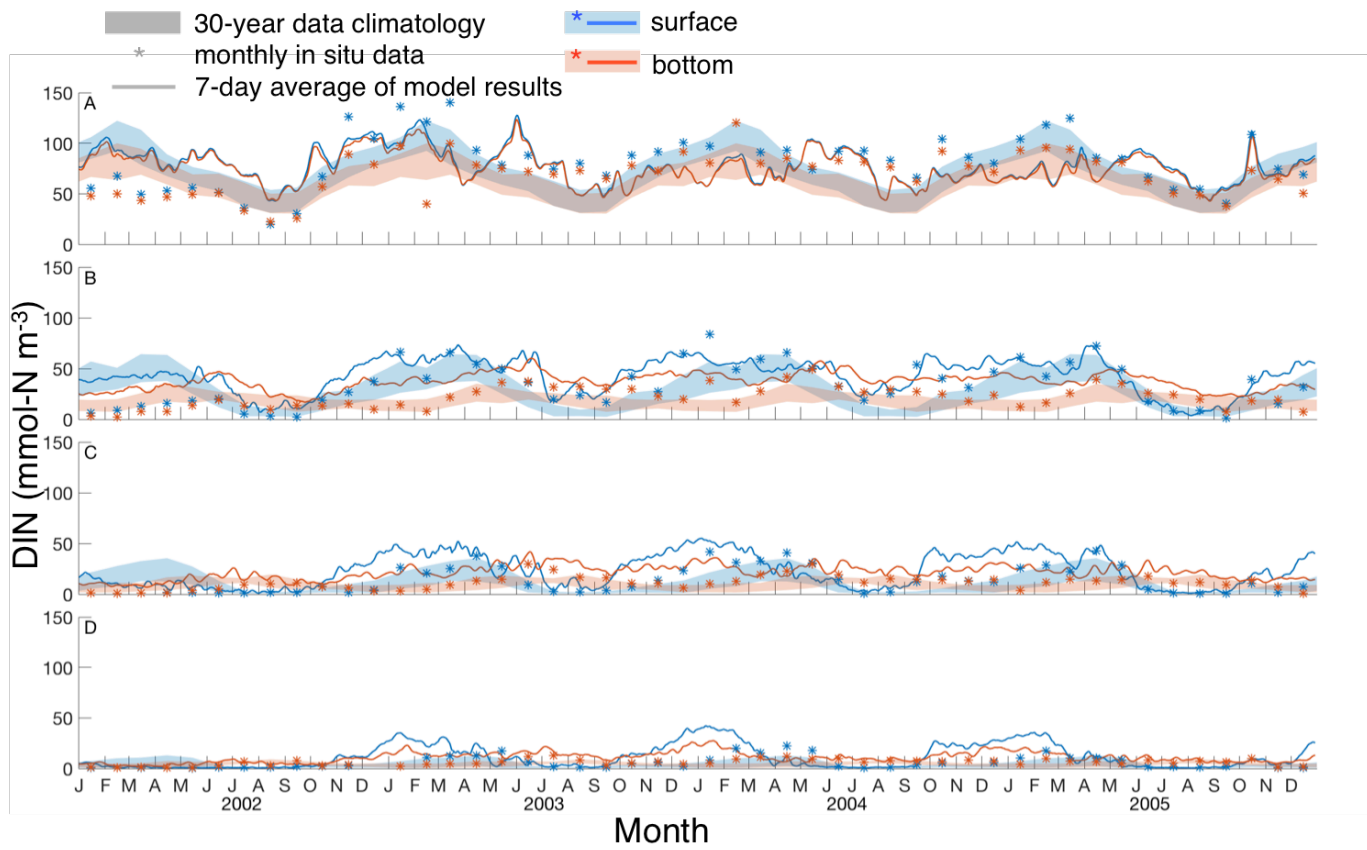


**Figure B5.** As in Figure B2, but for DIN.

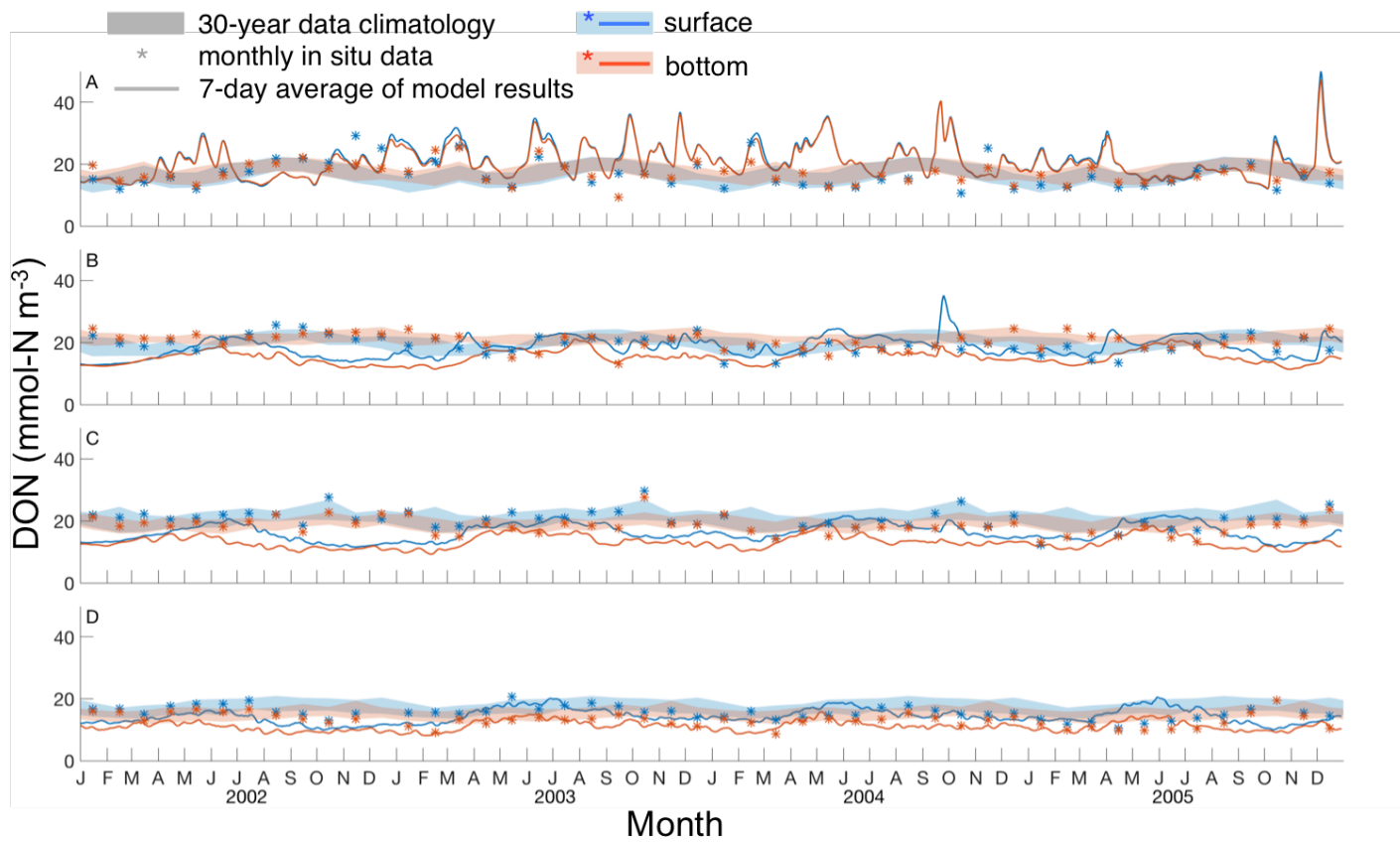


**Figure B6.** As in Figure B2, but for DON.

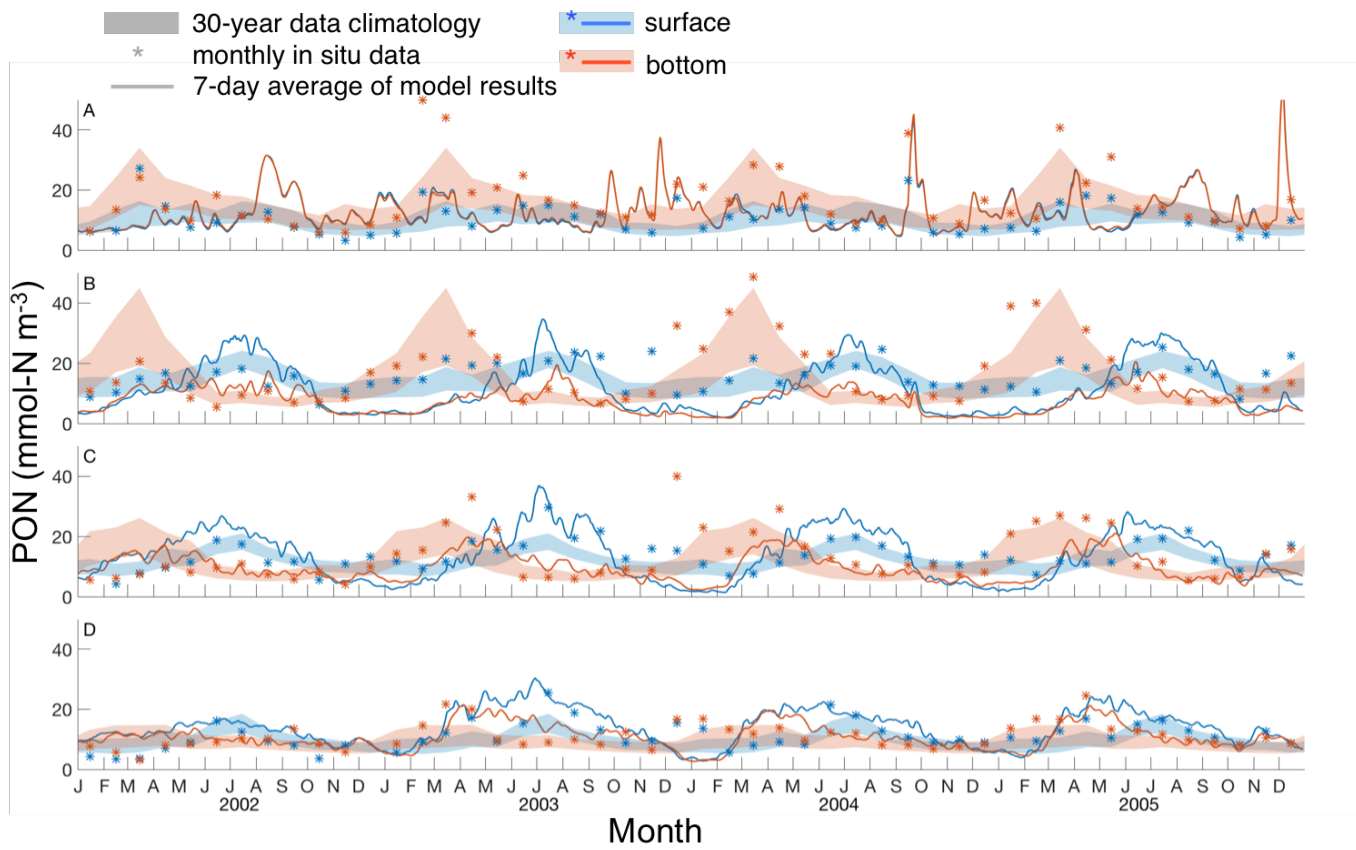


**Figure B7.** As in Figure B2, but for PON.

## References

Ator, S.W., & Denver, J.M. (2015). Understanding nutrients in the Chesapeake Bay watershed and implications for management and restoration—the Eastern Shore (ver. 1.2, June 2015). U.S. Geological Survey Circular 1406, 72 p.

<http://dx.doi.org/10.3133/cir1406>

Appel, K. W., Pouliot, G. A., Simon, H., Sarwar, G., Pye, H. O. T., Napelenok, S. L., et al. (2013). Evaluation of dust and trace metal estimates from the community multiscale air quality (CMAQ) model version 5.0. *Geoscientific Model Development*, 6, 883.

<https://doi.org/10.5194/gmd-6-883-2013>

Bever, A. J., Friedrichs, M. A. M., Friedrichs, C. T., Scully, M. E., & Lanerolle, L. W. (2013). Combining observations and numerical model results to improve estimates of hypoxic volume within the Chesapeake Bay, USA. *Journal of Geophysical Research: Oceans*, 118(10), 4924-4944. <http://doi.org/10.1002/jgrc.20331>

Blanton, J. O., Schwing, F. B., Weber, A. H., Pietrafesa, L. J., & Hayes, D. W. (1985) Wind Stress Climatology in the South Atlantic Bight, in *Oceanography of the Southeastern U.S. Continental Shelf* (eds L. P. Atkinson, D. W. Menzel and K. A. Bush). Washington, DC: American Geophysical Union. <http://doi.org/10.1029/CO002p0010>

Bronk, D. A., Glibert, P. M., Malone, T. C., Banahan, S., & Sahlsten, E. (1998). Inorganic and organic nitrogen cycling in Chesapeake Bay: Autotrophic versus heterotrophic processes and relationships to carbon flux. *Aquatic Microbial Ecology*, 15(2), 177-189.

Brown, C. A., & Ozretich, R. J. (2009). Coupling between the coastal ocean and Yaquina Bay, Oregon: Importance of oceanic inputs relative to other nitrogen sources. *Estuaries and Coasts*, 32(2), 219-237. <https://doi.org/10.1007/s12237-008-9128-6>

Cerco, C. and Noel, M. (2017). The 2017 Chesapeake Bay Water Quality and Sediment Transport Model. U.S. Army Engineer Waterways Experiment Station, Vicksburg MS. [https://www.chesapeakebay.net/documents/2017\\_WQSTM\\_Documentation\\_DRAFT\\_5-10-17.pdf](https://www.chesapeakebay.net/documents/2017_WQSTM_Documentation_DRAFT_5-10-17.pdf)

Davis, K. A., Banas, N. S., Giddings, S. N., Siedlecki, S. A., MacCready, P., Lessard, E. J., et al. (2014). Estuary-enhanced upwelling of marine nutrients fuels coastal productivity in the U.S. Pacific Northwest. *Journal of Geophysical Research: Oceans*, 119(12), 8778-8799. <http://doi.org/10.1002/2014JC010248>

Diaz, R. J., & Rosenberg, R. (1995). Marine benthic hypoxia: A review of its ecological effects and the behavioural responses of benthic macrofauna. *Oceanography and Marine Biology. an Annual Review*, 33, 245-203.

Eppley, R. W. (1972). Temperature and phytoplankton growth in the sea. *Fishery Bulletin*, 70, 1063-1085.

Feng, Y., Friedrichs, M.A., Wilkin, J., Tian, H., Yang, Q., Hofmann, E.E., et al. (2015). Chesapeake Bay nitrogen fluxes derived from a land-estuarine ocean biogeochemical modeling system: Model description, evaluation, and nitrogen budgets. *Journal of Geophysical Research: Biogeosciences*, 120(8), 1666-1695. <http://doi.org/10.1002/2015JG002931>

Filippino, K.C., Bernhardt, P.W. & Mulholland, M.R. (2009). Chesapeake Bay plume morphology and the effects on nutrient dynamics and primary productivity in the coastal zone. *Estuaries and Coasts*, 32(3), 410-424. <https://doi.org/10.1007/s12237-009-9139-y>

Fisher, D. C., & Oppenheimer, M. (1991). Atmospheric nitrogen deposition and the Chesapeake Bay estuary. *Ambio*, 20(3/4), 102-108. <http://www.jstor.org/stable/4313793>

- Fisher, T.R., Hagy, J.D., & Rochelle-Newall, E. (1998). Dissolved and particulate organic carbon in Chesapeake Bay. *Estuaries*, 21(2), 215-229.  
<https://doi.org/10.2307/1352470>
- Fisher, T., Gustafson, A., Sellner, K., et al (1999). Spatial and temporal variation of resource limitation in Chesapeake Bay. *Marine Biology*, 133(4), 763-778.  
<https://doi.org/10.1007/s002270050518>
- Gantt, B., Kelly, J. T., & Bash J. (2015). Updating sea spray aerosol emissions in the Community Multiscale Air Quality (CMAQ) model version 5.0.2, *Geoscientific Model Development*, 8, 3733–3746. <http://doi.org/10.5194/gmd-8-3733-2015>
- Geyer, W. R. (2010), Estuarine salinity structure and circulation, in *Contemporary Issues in Estuarine Physics*, edited by A. Valle-Levinson, pp. 12–26, Cambridge Univ., Cambridge, U. K.
- Grimm, J., & Lynch, J. (2005). Improved daily precipitation nitrate and ammonium concentration models for the Chesapeake Bay watershed. *Environmental Pollution*, 135(3), 445-455. <https://doi.org/10.1016/j.envpol.2004.11.018>
- Grimm, J. (2017). Extension of ammonium and nitrate wet-fall deposition models for the Chesapeake Bay watershed. The Pennsylvania State University.  
([ftp://ftp.chesapeakebay.net/modeling/Phase6/Draft\\_Phase\\_6/Documentation/03H%20Final\\_Report\\_Extension\\_of\\_Ammonium\\_and\\_Nitrate\\_Wet-Fall\\_Deposition\\_Models\\_for\\_the\\_CBW\\_Jan2017.pdf](ftp://ftp.chesapeakebay.net/modeling/Phase6/Draft_Phase_6/Documentation/03H%20Final_Report_Extension_of_Ammonium_and_Nitrate_Wet-Fall_Deposition_Models_for_the_CBW_Jan2017.pdf))
- Hagy, J. D., Boynton, W. R., Keefe, C. W., & Wood, K. V. (2004). Hypoxia in Chesapeake Bay, 1950–2001: Long-term change in relation to nutrient loading and river flow. *Estuaries*, 27(4), 634-658. <https://doi.org/10.1007/BF02907650>

Hagy, J. D., Boynton, W. R., & Jasinski, D. A. (2005). Modelling phytoplankton deposition to Chesapeake Bay sediments during winter–spring: Interannual variability in relation to river flow. *Estuarine, Coastal and Shelf Science*, 62(1-2), 25-40. <https://doi.org/10.1016/j.ecss.2004.08.004>

Harding, L. W., Mallonee, M. E., & Perry, E. S. (2002). Toward a predictive understanding of primary productivity in a temperate, partially stratified estuary. *Estuarine, Coastal and Shelf Science*, 55(3), 437-463. <https://doi.org/10.1006/ecss.2001.0917>

Harding, L. W., Gallegos, C., Perry, E., Miller, W., Adolf, J., Mallonee, M., & Paerl, H. W. (2016). Long-term trends of nutrients and phytoplankton in Chesapeake Bay. *Estuaries and Coasts*, 39(3), 664-681. <https://doi.org/10.1007/s12237-015-0023-7>

Hickey, B. M., & Banas, N. S. (2003). Oceanography of the US Pacific Northwest coastal ocean and estuaries with application to coastal ecology. *Estuaries*, 26(4), 1010-1031. <https://doi.org/10.1007/BF02803360>

Hinga, K. R., Keller, A. A., & Oviatt, C. A. (1991). Atmospheric deposition and nitrogen inputs to coastal waters. *Ambio*, 20(6), 256-260. <http://www.jstor.org/stable/4313835>

Hofmann, E., Druon, J., Fennel, K., Friedrichs, M. A. M., Haidvogel, D., Lee, C., et al. (2008). Eastern US continental shelf carbon budget integrating models, data assimilation, and analysis. *Oceanography*, 21(1), 86–104. <http://dx.doi.org/10.5670/oceanog.2008.70>

Holland, A., Shaughnessy, A. T., & Hiegel, M. H. (1987). Long-term variation in mesohaline Chesapeake Bay macrobenthos: Spatial and temporal patterns. *Estuaries*, 10(3), 227-245. <http://doi.org/10.2307/1351851>

Irby, I. D., Friedrichs, M. A. M., Friedrichs, C. T., Bever, A. J., Hood, R. R., Lanerolle, L. W., & Scully, M. E. (2016). Challenges associated with modeling low-oxygen waters in Chesapeake Bay: A multiple model comparison. *Biogeosciences*, 13(7), 2011. <https://doi.org/10.5194/bg-13-2011-2016>

Irby, I. D., Friedrichs, M. A. M., Da, F. and Hinson, K. E. (2017). The competing impacts of climate change and nutrient reductions on dissolved oxygen in Chesapeake Bay. *Biogeosciences Discussions*, in review. <http://doi.org/10.5194/bg-2017-416>

Janowitz, G. S., & Pietrafesa, L. J. (1982). The effects of alongshore variation in bottom topography on a boundary current—(topographically induced upwelling). *Continental Shelf Research*, 1(2), 123-141. [https://doi.org/10.1016/0278-4343\(82\)90001-2](https://doi.org/10.1016/0278-4343(82)90001-2)

Jerlov, N.G. (1976). *Marine Optics. Elsevier Oceanography Series*. (Vol. 14). Amsterdam, Netherlands: Elsevier.

Jolliff, J. K., Kindle, J. C., Shulman, I., Penta, B., Friedrichs, M. A. M., Helber, R., & Arnone, R. A. (2009). Summary diagrams for coupled hydrodynamic-ecosystem model skill assessment. *Journal of Marine Systems*, 76(1-2), 64-82. <https://doi.org/10.1016/j.jmarsys.2008.05.014>

Keene, W., Montag, J., Maben, J., Southwell, M., Leonard, J., Church, T., et al. (2002). Organic nitrogen in precipitation over Eastern North America. *Atmospheric Environment*, 36(28), 4529-4540. [https://doi.org/10.1016/S1352-2310\(02\)00403-X](https://doi.org/10.1016/S1352-2310(02)00403-X)

Kemp, W. M., Smith, E. M., Marvin-DiPasquale, M. M., & Boynton W. R. (1997). Organic carbon balance and net ecosystem metabolism in Chesapeake Bay, *Marine Ecology Progress Series*, 150, 229-248. <https://doi.org/10.3354/meps150229>



Kemp, W. M., Boynton, W. R., Adolf, J. E., Boesch, D. F., Boicourt, W. C., Brush, G., et al. (2005). Eutrophication of Chesapeake Bay: Historical trends and ecological interactions. *Marine Ecology Progress Series*, 303, 1-29. <http://doi.org/10.3354/meps303001>

Kremer, J. N., & Nixon, S. W. (1978). *A coastal marine ecosystem, simulation and analysis*. New York: Springer-Verlag.

Li, M., Lee, Y. J., Testa, J. M., Li, Y., Ni, W., Kemp, W. M., & Di Toro, D. M. (2016). What drives interannual variability of hypoxia in Chesapeake Bay: Climate forcing versus nutrient loading? *Geophysical Research Letters*, 43, 2127–2134. <http://doi.org/10.1002/2015GL067334>

Li, Y., Schichtel, B. A., Walker, J. T., Schwede, D. B., Chen, X., Lehmann, C. M., et al. (2016). Increasing importance of deposition of reduced nitrogen in the United States. *Proceedings of the National Academy of Sciences of the United States of America*, 113(21), 5874-5879. <https://doi.org/10.1073/pnas.1525736113>

Linker, L. C., Dennis, R., Shenk, G. W., Batiuk, R. A., Grimm, J., & Wang, P. (2013). Computing atmospheric nutrient loads to the Chesapeake Bay watershed and tidal waters. *JAWRA Journal of the American Water Resources Association*, 49(5), 1025-1041. <http://doi.org/10.1111/jawr.12112>

Lomas, M.W., Gilbert, P.M., Shiah, F.K., & Smith, E.M. (2002). Microbial processes and temperature in Chesapeake Bay: current relationships and potential impacts of regional warming, *Global Change Biology*, 8(1), 51-70. <http://doi.org/10.1046/j.1365-2486.2002.00454.x>

Mannino, A., Signorini, S. R., Novak, M. G., Wilkin, J., Friedrichs, M. A. M., & Najjar, R. G. (2016). Dissolved organic carbon fluxes in the Middle Atlantic Bight: An integrated approach based on satellite data and ocean model products. *Journal of Geophysical Research: Biogeosciences*, 121(2), 312-336.

<http://doi.org/10.1002/2015JG003031>

Marchesiello, P., McWilliams, J., & Shchepetkin, A. (2001). Open boundary conditions for long-term integration of regional oceanic models. *Ocean Modelling*, 3(1-2), 1-20.

[https://doi.org/10.1016/S1463-5003\(00\)00013-5](https://doi.org/10.1016/S1463-5003(00)00013-5)

Melrose, D.C., Rebeck, N.D., Townsend, D. W., Thomas, M., & Taylor, C. (2015). Ammonia, silicate, phosphate, nitrite+nitrate, dissolved oxygen, and other variables collected from profile and discrete sample observations using CTD, nutrient autoanalyzer, and other instruments from NOAA Ship Delaware II, NOAA Ship Gordon Gunter, NOAA Ship Henry B. Bigelow, NOAA Ship Okeanos Explorer, and NOAA Ship Pisces in the Gulf of Maine, Georges Bank, and Mid-Atlantic Bight from 2009-11-03 to 2016-08-19 (NCEI Accession 0127524). Version 9.9. NOAA National Centers for Environmental Information. Dataset. doi:10.7289/V5HQ3WV3

Mesinger, F., DiMego, G., Kalnay, E., Mitchell, K., Shafran, P. C., Ebisuzaki, W., et al. (2006): North American Regional Reanalysis. *Bulletin of the American Meteorological Society*, 87, 343–360. <https://doi.org/10.1175/BAMS-87-3-343>

Moriarty, J. M., Harris, C. K., Fennel, K., Friedrichs, M. A. M., Xu, K., & Rabouille, C. (2017). The roles of resuspension, diffusion and biogeochemical processes on oxygen dynamics offshore of the Rhône River, France: a numerical modeling study. *Biogeosciences*, 14, 1919-1946. <https://doi.org/10.5194/bg-14-1919-2017>, 2017

Murphy, R. R., Kemp, W. M., & Ball, W. P. (2011). Long-term trends in Chesapeake Bay seasonal hypoxia, stratification, and nutrient loading. *Estuaries and Coasts*, 34(6), 1293-1309. <https://doi.org/10.1007/s12237-011-9413-7>

National Atmospheric Deposition Program (NRSP-3). 2017. NADP Program Office, Illinois State Water Survey, University of Illinois, Champaign, IL.

Newcombe, C. L., & Horne, W. A. (1938). Oxygen-poor waters of the Chesapeake Bay. *Science*, 88(2273), 80-81. <http://doi.org/10.1126/science.88.2273.80>

Nixon, S. W. (1995). Coastal marine eutrophication: A definition, social causes, and future concerns. *Ophelia*, 41(1), 199-219.  
<http://doi.org/10.1080/00785236.1995.10422044>

Paerl, Hans W. (1997). Coastal eutrophication and harmful algal blooms: Importance of atmospheric deposition and groundwater as “new” nitrogen and other nutrient sources. *Limnology and Oceanography*, 42, 1154-1165.  
[http://doi.org/10.4319/lo.1997.42.5\\_part\\_2.1154](http://doi.org/10.4319/lo.1997.42.5_part_2.1154)

Paerl, H. W., Willey, J. D., Go, M., Peierls, B. L., Pinckney, J. L., & Fogel, M. L. (1999). Rainfall stimulation of primary production in western Atlantic Ocean waters: Roles of different nitrogen sources and co-limiting nutrients. *Marine Ecology Progress Series*, 76, 205–214.

Paerl, H. W., Dennis, R. L., & Whittall, D. R. (2002). Atmospheric deposition of nitrogen: Implications for nutrient over-enrichment of coastal waters. *Estuaries*, 25(4b), 677-693.  
<https://doi.org/10.1007/BF02804899>

Paulson, C. A., & Simpson, J. J. (1977): Irradiance measurements in the upper ocean. *Journal of Physical Oceanography*, 7, 952-956. [https://doi.org/10.1175/1520-0485\(1977\)007<0952:IMITUO>2.0.CO;2](https://doi.org/10.1175/1520-0485(1977)007<0952:IMITUO>2.0.CO;2)

Pietrafesa, L., Morrison, J. M., McCann, M., Churchill, J., Böhm, E., & Houghton, R. (1994). Water mass linkages between the Middle and South Atlantic Bights. *Deep Sea Research Part II: Topical Studies in Oceanography*, 41(2), 365-389. [https://doi.org/10.1016/0967-0645\(94\)90028-0](https://doi.org/10.1016/0967-0645(94)90028-0)

Prospero, J., Barrett, K., Church, T., Dentener, F., Duce, R., Galloway, J., et al. (1996). Atmospheric deposition of nutrients to the North Atlantic Basin. *Biogeochemistry*, 35(1), 27-73. <https://doi.org/10.1007/BF02179824>

Najjar, R. G., Herrmann, M., Aleander, R., Boyer, E.W., Burdige, D., Butman, D., et al. (2018). Carbon budget of tidal wetlands, estuaries, and shelf waters of Eastern North America. *Global Biogeochemical Cycles*, 32. <https://doi.org/10.1002/2017GB005790>

Russell, K. M., Galloway, J. N., Macko, S. A., Moody, J. L., & Scudlark, J. R. (1998). Sources of nitrogen in wet deposition to the Chesapeake Bay region. *Atmospheric Environment*, 32(14), 2453-2465. [https://doi.org/10.1016/S1352-2310\(98\)00044-2](https://doi.org/10.1016/S1352-2310(98)00044-2)

Sarwar, G., Godowitch, J., Henderson, B., Fahey, K., Pouliot, G., Bill Hutzell, et al. (2013). A comparison of atmospheric composition using the Carbon Bond and Regional Atmospheric Chemistry Mechanisms. *Atmospheric Chemistry and Physics*, 13(19), 9675-9712.

Schwede, D.B., & Lear, G.G. (2014). A novel hybrid approach for estimating total deposition in the United States. *Atmospheric Environment*, 92, 207-220. <https://doi.org/10.1016/j.atmosenv.2014.04.008>

Scully, M. E. (2013). Physical controls on hypoxia in Chesapeake Bay: A numerical modeling study. *Journal of Geophysical Research: Oceans*, 118(3), 1239-1256. <http://doi.org/10.1002/jgrc.20138>

Scully, M. E. (2016). Mixing of dissolved oxygen in Chesapeake Bay driven by the interaction between wind-driven circulation and estuarine bathymetry. *Journal of Geophysical Research: Oceans*, 121(8), 5639-5654.

<http://doi.org/10.1002/2016JC011924>

Seliger, H. H., Boggs, J. A., & Biggley, W. H. (1985). Catastrophic anoxia in the Chesapeake Bay in 1984. *Science*, 228(4695). <http://doi.org/70-73.228/4695/70>

Shchepetkin, A., & McWilliams, J. (2005). The regional ocean modeling system (ROMS): A split-explicit, free-surface, topography-following-coordinate ocean model. *Ocean Modeling*, 9, 347–404. <https://doi.org/10.1016/j.ocemod.2004.08.002>

Shenk, G. W., & Linker, L. C. (2013). Development and application of the 2010 Chesapeake Bay watershed total maximum daily load model. *JAWRA Journal of the American Water Resources Association*, 49(5), 1042-1056.

<http://doi.org/10.1111/jawr.12109>

Shiah, F. K., & H. W. Ducklow. (1994). Temperature regulation of heterotrophic bacterioplankton abundance, production, and specific growth rate in Chesapeake Bay. *Limnology and Oceanography*, 39, 1243-1258. <http://doi.org/10.4319/lo.1994.39.6.1243>

Skamarock, W. C., Klemp, J. B., Dudhia, J., Gill, D. O., Barker, D. M., Dudha, M. G., et al. (2008). A description of the advanced research WRF Version 30, NCAR technical note, *Technical Report*, NCAR/TN-475.

Smolarkiewicz, P. K. (1983). A simple positive definite advection scheme with small implicit diffusion. *Monthly Weather Review*, 111(3), 479-486.

[https://doi.org/10.1175/1520-0493\(1983\)111<0479:ASPDAS>2.0.CO;2](https://doi.org/10.1175/1520-0493(1983)111<0479:ASPDAS>2.0.CO;2)

Smolarkiewicz, P. K. (1984). A fully multidimensional positive definite advection transport algorithm with small implicit diffusion. *Journal of Computational Physics*, 54(2), 325-362. [https://doi.org/10.1016/0021-9991\(84\)90121-9](https://doi.org/10.1016/0021-9991(84)90121-9)

Son, S., Wang, M., & Harding, L. W. (2014). Satellite-measured net primary production in the Chesapeake Bay. *Remote Sensing of Environment*, 144, 109-119. <https://doi.org/10.1016/j.rse.2014.01.018>

St-Laurent, P., Friedrichs, M. A. M., Najjar, R. G., Martins, D. K., Herrmann, M., Miller, S. K., & Wilkin, J. (2017). Impacts of atmospheric nitrogen deposition on surface waters of the Western North Atlantic mitigated by multiple feedbacks. *Journal of Geophysical Research: Oceans*, 122(11), 8406-8426. <http://doi.org/10.1002/2017JC013072>

Testa, J.M., & Kemp, W.M. (2014). Spatial and temporal patterns of winter–spring oxygen depletion in Chesapeake Bay bottom water. *Estuaries and Coasts*, 37(6), 1432-1448. <https://doi.org/10.1007/s12237-014-9775-8>

Tian, H., Yang, Q., Najjar, R. G., Ren, W., Friedrichs, M. A. M., Hopkinson, C. S., & Pan, S. (2015). Anthropogenic and climatic influences on carbon fluxes from eastern North America to the Atlantic Ocean: A process-based modeling study, *Journal of Geophysical Research: Biogeosciences*, 120, 752–772. <http://doi.org/10.1002/2014JG002760>

Townsend, D. W., Thomas, A. C., Mayer, L. M., Thomas, M. A., & Quinlan, J. A. (2006). Oceanography of the Northwest Atlantic Continental Shelf. In A.R. Robinson, K.H. Brink (Eds.), *The Sea* (Vol. 14A, pp. 119-168). Cambridge, MA: Harvard University Press.

USEPA (U.S. Environmental Protection Agency). (2010a). Chesapeake Bay Total Maximum Daily Load for Nitrogen, Phosphorus and Sediment Appendix L: Setting the Chesapeake Bay Atmospheric Nitrogen Deposition Allocations. U.S. Environmental Protection Agency, Chesapeake Bay Program Office, Annapolis, Maryland.  
[http://www.epa.gov/reg3wapd/pdf/pdf\\_chesbay/FinalBayTMDL/AppendixLAtmosNDepositionAllocations\\_final.pdf](http://www.epa.gov/reg3wapd/pdf/pdf_chesbay/FinalBayTMDL/AppendixLAtmosNDepositionAllocations_final.pdf).

USEPA (U.S. Environmental Protection Agency). (2010b). Chesapeake Bay Phase 5.3 Community Watershed Model: Section 1. Phase 5.3 Watershed Model Overview. U.S. Environmental Protection Agency, Chesapeake Bay Program Office, Annapolis, Maryland.  
[ftp://ftp.chesapeakebay.net/modeling/P5Documentation/SECTION\\_1.pdf](ftp://ftp.chesapeakebay.net/modeling/P5Documentation/SECTION_1.pdf).

USEPA (U.S. Environmental Protection Agency). (2010c). Chesapeake Bay Phase 5.3 Community Watershed Model: Section 11. Simulation and Calibration of Riverine Fate and Transport of Nutrients and Sediment. U.S. Environmental Protection Agency, Chesapeake Bay Program Office, Annapolis, Maryland.  
[ftp://ftp.chesapeakebay.net/Modeling/P5Documentation/SECTION\\_11.pdf](ftp://ftp.chesapeakebay.net/Modeling/P5Documentation/SECTION_11.pdf).

Williams, R. G., McDonagh, E., Roussenov, V. M., Torres-Valdes, S., King, B., Sanders, R., & Hansell, D. A. (2011). Nutrient streams in the North Atlantic: Advective pathways of inorganic and dissolved organic nutrients. *Global Biogeochemical Cycles*, 25(4), GB4008. <http://doi.org/10.1029/2010GB003853>

Xia, Y., Mitchell, K., Ek, M., Sheffield, J., Cosgrove, B., Wood, E., et al. (2012). Continental-scale water and energy flux analysis and validation for the North American Land Data Assimilation System project phase 2 (NLDAS-2): 1. intercomparison and application of model products. *Journal of Geophysical Research: Atmospheres*, 117(D3), D03109. <http://doi.org/10.1029/2011JD016048>

Xiao, Y., & Friedrichs, M.A.M. (2014a). Using biogeochemical data assimilation to assess the relative skill of multiple ecosystem models: effects of increasing the complexity of the planktonic food web. *Biogeosciences*, 11, 3015-3030.  
<http://doi.org/10.5194/bg-11-3015-2014>

Xiao, Y. & Friedrichs, M.A.M. (2014b). The assimilation of satellite-derived data into a one-dimensional lower trophic level marine ecosystem model. *Journal of Geophysical Research-Oceans*, 119, 2691-2712, <http://doi:10.1002/2013JC009433>

Xu, J., Long, W., Wiggert, J. D., Lanerolle, L. W. J., Brown, C. W., Murtugudde, R., & Hood, R. R. (2012). Climate forcing and salinity variability in Chesapeake Bay, USA. *Estuarine Coastal Shelf Science*, 35(1), 237–261. <https://doi.org/10.1007/s12237-011-9423-5>